NASA/TM–1999-208790

An Experimental Study of Parallel Blade-Vortex Interaction Aerodynamics and Acoustics Utilizing an Independently Generated Vortex

C. Kitaplioglu, F. X. Caradonna, and M. McCluer

July 1999

The NASA STI Program Office . . . in Profile

Since its founding, NASA has been dedicated to the advancement of aeronautics and space science. The NASA Scientific and Technical Information (STI) Program Office plays a key part in helping NASA maintain this important role.

The NASA STI Program Office is operated by Langley Research Center, the Lead Center for NASA's scientific and technical information. The NASA STI Program Office provides access to the NASA STI Database, the largest collection of aeronautical and space science STI in the world. The Program Office is also NASA's institutional mechanism for disseminating the results of its research and development activities. These results are published by NASA in the NASA STI Report Series, which includes the following report types:

- TECHNICAL PUBLICATION. Reports of completed research or a major significant phase of research that present the results of NASA programs and include extensive data or theoretical analysis. Includes compilations of significant scientific and technical data and information deemed to be of continuing reference value. NASA's counterpart of peer-reviewed formal professional papers but has less stringent limitations on manuscript length and extent of graphic presentations.
- TECHNICAL MEMORANDUM. Scientific and technical findings that are preliminary or of specialized interest, e.g., quick release reports, working papers, and bibliographies that contain minimal annotation. Does not contain extensive analysis.
- CONTRACTOR REPORT. Scientific and technical findings by NASA-sponsored contractors and grantees.
- CONFERENCE PUBLICATION. Collected papers from scientific and technical conferences, symposia, seminars, or other meetings sponsored or cosponsored by NASA.
- SPECIAL PUBLICATION. Scientific, technical, or historical information from NASA programs, projects, and missions, often concerned with subjects having substantial public interest.
- TECHNICAL TRANSLATION. English-language translations of foreign scientific and technical material pertinent to NASA's mission.

Specialized services that complement the STI Program Office's diverse offerings include creating custom thesauri, building customized databases, organizing and publishing research results . . . even providing videos.

For more information about the NASA STI Program Office, see the following:

- Access the NASA STI Program Home Page at *http://www.sti.nasa.gov*
- E-mail your question via the Internet to help@sti.nasa.gov
- Fax your question to the NASA Access Help Desk at (301) 621-0134
- Telephone the NASA Access Help Desk at (301) 621-0390
- Write to:
  NASA Access Help Desk
  NASA Center for AeroSpace Information
  7121 Standard Drive
  Hanover, MD 21076-1320

NASA/TM–1999-208790

An Experimental Study of Parallel Blade-Vortex Interaction Aerodynamics and Acoustics Utilizing an Independently Generated Vortex

C. Kitaplioglu, F. X. Caradonna, and M. McCluer
Ames Research Center, Moffett Field, California

National Aeronautics and
Space Administration

Ames Research Center
Moffett Field, California 94035-1000

July 1999

Acknowledgments

The authors wish to acknowledge the invaluable assistance of Cdr. Steve Christiansen and Mr. Steve Craft, who served as Test Directors, responsible for the overall operational execution of this test program.

Available from:

NASA Center for AeroSpace Information
7121 Standard Drive
Hanover, MD 21076-1320
(301) 621-0390

National Technical Information Service
5285 Port Royal Road
Springfield, VA 22161
(703) 487-4650

CONTENTS

Summary 1

Nomenclature 1

Introduction 2

Test Objective 3

Description of Experiment 3

Background 3

Rotor and Test Stand 4

Vortex Generator 5

Microphones 5

Wind Tunnel Installation 6

Test Procedures 6

Data Acquisition 7

Data Processing 8

Blade Pressure Data 8

Acoustic Data 8

Description of Data 9

References 10

Table 11

Figures 12

Appendices 15

AN EXPERIMENTAL STUDY OF PARALLEL BLADE-VORTEX INTERACTION AERODYNAMICS AND ACOUSTICS UTILIZING AN INDEPENDENTLY GENERATED VORTEX

C. Kitaplioglu, F. X. Caradonna, and M. McCluer

Ames Research Center

SUMMARY

This report presents results from an experimental study of rotor blade-vortex interaction (BVI) aerodynamics and acoustics. The experiment utilized an externally generated vortex interacting with a two-bladed rotor operating at zero thrust to minimize the influence of the rotor's own wake. The rotor blades were instrumented with a total of 60 absolute pressure transducers at three spanwise and ten chordwise stations on both the upper and lower surfaces. Acoustic data were obtained with fixed near-field microphones as well as a movable array of far-field microphones. The test was carried out in the acoustically treated test section of the NASA Ames 80- by 120-Foot Wind Tunnel. Several parameters that influence BVI, such as vortex-rotor separation distance, vortex strength, and vortex sense (swirl direction), as well as rotor tip Mach number and advance ratio, were varied. Simultaneous measurements were obtained of blade surface pressure distributions, near-field acoustics, and far-field acoustics during the vortex-blade encounters. A representative subset of the data is included in the Appendices. The entire reduced data set is included on the enclosed CD-ROM.

NOMENCLATURE

a_0	speed of sound (ft/sec)
c	blade chord (in)
$C_p = (p - p_s)/0.5*\rho*V_\infty{}^2$	pressure coefficient
C_T/σ	rotor thrust coefficient/rotor solidity
c_v	vortex generator wing chord
$L_p = 20 \log_{10}(p/p_{ref})$	Sound Pressure Level (dB)
M_{tip}	hover tip Mach number
p	pressure
p_{ref}	reference acoustic pressure (2×10^{-5} Pascals)
p_s	static pressure (psi)

R	rotor radius (in)
T_T	wind tunnel test section total temperature (°F)
V_∞	tunnel free stream velocity (ft/sec)
x_m	microphone traverse streamwise location
x, y, z	coordinate system centered on the rotor hub
z_v	vertical vortex location relative to rotor plane (in)
α_v	vortex generator angle of attack (deg)
Γ_v	vortex circulation (ft^2/sec)
ζ_v	nondimensional core size (ratio of maximum tangential velocity radius/vortex generator chord)
θ_c	rotor collective pitch (deg)
μ	rotor advance ratio
ρ	density (slug/ft^2)
ϕ	elevation angle measured positive down from rotor plane (deg)
ψ	azimuth angle measured positive in rotation direction; $\psi = 0$ downstream (deg)

INTRODUCTION

The interaction of a rotor with one or more of its tip vortices can occur in many forms and is a topic of considerable interest. Such interactions are a primary source of rotor vibratory loading and rotorcraft noise. When the rotor blade and the tip vortex are very close and nearly parallel to each other, the interaction is particularly strong (though of short duration). This type of interaction is usually referred to as a parallel blade-vortex interaction (BVI) and is the subject of this experimental investigation.

A large number of aerodynamic and acoustic computational codes (refs. 1–5), embodying a wide range of physical models of BVI, have been developed. The aerodynamic models range from two-dimensional (2-D), ideal-flow, “vortex-cloud” methods employing conformal mapping solutions to three-dimensional (3-D), compressible Euler/Navier-Stokes computational fluid dynamics (CFD) methods—with the middle ground being held by 3-D full-potential CFD methods. Acoustic prediction methods are of two types: the acoustic analogy methods (e.g., ref. 2) and the more recent Kirchhoff methods (e.g., ref. 4). CFD methods can also be used for acoustic prediction but cannot yet be extended to the far-field with which acoustics is ultimately concerned. Nevertheless, CFD has great potential for providing input for acoustic prediction methods. The choice between these methods is dependent on the extent to which flow-field nonlinearity dominates the solution. The aerodynamics of the near-field is of critical importance both for determining the essential physics and the type of acoustic method that must be used. Developing combined aeroacoustic computational methods in which we have high confidence is crucially important. Such confidence requires validation using the simplest possible tests. Until the present, however, most BVI aeroacoustic tests have involved the use of rotor models operating at typical flight conditions. The complexities of typical rotor flows (with wake geometries whose strengths and locations with respect to the blade are difficult to determine) are considerable. The present work took a different experimental approach. Rather than operating a rotor under typical flight conditions generating complex BVI, the simplest possible interaction geometry was experimentally created that is easily modeled in most CFD codes. In effect, rather than refining the computational model to account for real world complexities, we have attempted to refine the experiment to reflect the simplest possible computational model of BVI upon which the prediction codes ultimately depend. If the codes cannot do a good job of correlating with a simplified experiment, there is little reason to expect good correlation with real flight data.

This report describes the wind tunnel experiment designed to investigate the fundamentals of BVI aeroacoustics and presents representative blade pressure and acoustic data.

TEST OBJECTIVE

The objective of the test was to experimentally simulate the aerodynamics and acoustics of parallel, unsteady BVI. In particular, it was desired to set up an experiment that matched, as closely as possible, the simplified 2-D model of a rotor blade undergoing an unsteady, parallel interaction with a vortex, as illustrated in figure 1.

DESCRIPTION OF EXPERIMENT

Background

The test was performed in the NASA Ames 80- by 120-Foot Wind Tunnel using the U.S. Army Rotary Wing Test Stand (RWTS).

To provide independent control of the interaction parameters, the vortex was generated separately by a wing tip, placed upstream of the rotor, and set at an angle of attack. The rotor was operated at zero thrust to minimize the generation of the rotor's own wake/tip-vortex system. The relative orientation of the rotor and wing ensured parallelism of the interaction. Figures 2 and 3 illustrate the experimental arrangement. Two similar experiments were previously performed by Caradonna (refs. 6–8); however, that work focused on the aerodynamic aspects of the problem and did not include acoustic measurements because the wind tunnel utilized had acoustically reflective walls. The present experiment extended that work to include acoustic studies.

This is a practical way to approximate a 2-D, unsteady interaction, although the complication of rotational and 3-D tip effects is introduced. Since the latter are important for rotors, this is not felt to be a serious shortcoming of the experiment. Codes specifically applicable to rotors will be expected to account for these effects. Alternative methods (refs. 9 and 10) of generating parallel, unsteady interactions are neither as amenable to control nor as repeatable as the present method. For example, to generate a parallel interaction using a fixed blade requires generation of either a periodic or an impulsive vortex. Both of these, although unsteady in nature, would be difficult to control and, most likely, have an unnecessarily complex core structure. In addition, this type of an experiment would require either a small wind tunnel or a complicated arrangement of end plates to maintain two-dimensionality, distinct disadvantages for acoustic measurements.

The major parameters expected to influence parallel, unsteady BVI are vortex strength and sense, determined by the vortex generator angle of attack (α_V), vortex-blade separation distance (z_V), rotor advance ratio (μ), and hover tip Mach number (M_{tip}). These parameters were all independently controlled in this experiment. The location of the vortex relative to the blade was measured using a laser sheet/high speed video system. The parallelism of the interaction was verified with a separate synchronized strobe and video camera that was located below the rotor. The blade surface pressures and the acoustic field were simultaneously measured for each specific interaction geometry. The surface pressure distribution was measured with a chordwise and spanwise array of transducers (fig. 4). Two sets of acoustic measurements were made. Two microphones in the near-field of the interaction provided information on the detailed evolution of the acoustic field and data to validate “mid-field” calculations of computational aeroacoustics and Kirchhoff methods. A movable array of microphones, at a distance of approximately three rotor radii from the rotor hub, was used to obtain a limited (due to time constraints) survey of the acoustic far-field.

Rotor and Test Stand

The test used a small-scale (7-foot diameter), two-bladed, teetering rotor. The blades are untwisted and have a rectangular planform with NACA 0012 airfoil section of 6-inch chord. The blade Reynolds number was of the order of 1,000,000. The blades are constructed of carbon composite material and are very stiff. Each blade is equipped with 30 absolute pressure transducers, one blade with upper surface transducers, the other with lower surface transducers. The transducers are distributed in three spanwise sets of ten chordwise locations. Figure 4 details the transducer locations. The transducers as installed had a flat frequency response up to 10 kHz.

The rotor was mounted on the RWTS, which is capable of driving the rotor up to 2300 RPM (tip Mach number of 0.75). Rotation was in the clockwise direction (when viewed from above the rotor). The long drive shaft was housed within an aerodynamic fairing covered with foam to minimize acoustic reflections. The RWTS has an internal six-component balance for measuring rotor loads and incorporates a 256-channel slip-ring assembly for routing blade safety and pressure transducer data. The RWTS also incorporates two encoders that provide 1/rev and 1024/rev TTL signals to facilitate data acquisition. The rotor controls consisted of an RPM control plus collective and cyclic pitch actuators that accepted direct input from a control box. Shaft angle was fixed at 0 deg.

Vortex Generator

The vortex was generated using a short rectangular wing with an 18-inch chord, a NACA 0015 airfoil, and a Reynolds number of the order of 600,000. The generated vortex had a core size of approximately 0.15 rotor blade chord. The wing is constructed in a two-piece telescoping arrangement to allow changes in vertical positioning of the vortex relative to the rotor blade. It had a total travel of 9 inches and was remotely controlled. The wing incorporates internal tubing to allow introduction of smoke near the tip for flow visualization. During this experiment, theatrical "fog juice" was used to make the vortex visible. The wing angle of attack (α_V) was manually set.

The vortex generator wing was mounted on an airfoil-shaped stand for placement at the appropriate height. The stand was constructed of perforated sheet metal covered with foam to prevent acoustic reflections. The interface between the stand and wing had provision for fine adjustment of lateral position (to ensure parallel interaction at the correct azimuth position of the rotor). The entire arrangement was designed to allow streamwise and lateral translation for studies of vortex age effects and oblique interactions.

Tip vortex strength and structure were not measured during this experiment. However, McAlister and Takahashi (ref. 11) conducted detailed laser velocimetry studies of a similarly generated vortex in the Army 7- by 10-Foot Wind Tunnel at Ames. Based on this experiment and some further studies (ref. 12), the vortex characteristics can be estimated as follows:

$$\Gamma_V = 0.374\ V_\infty\ c_V$$

$$\zeta_V = 0.054$$

Microphones

Two sets of microphones were installed for acoustic measurements. One set consisted of five microphones mounted at various heights on a remotely controlled traversing vertical strut. The traverse was mounted on the tunnel floor 10.04 feet to the starboard side of the RWTS and aligned with the flow. From the nominal "zero" position directly to the side of the rotor hub, the microphone strut could traverse upstream and downstream for distances of over 10 feet. This arrangement allowed placement of the vertical mic array at any azimuth angle between 225 and 315 deg relative to the rotor hub. In terms of standard rotor operation, this is equivalent to probing the forward advancing quadrant of the rotor. The five microphones were placed at elevation angles of 26, 32, 37, 43, and 47 deg (fig. 5) below the rotor hub (when the strut was in line with the hub). This arrangement provided a detailed map, for a limited number of test points, of the acoustic far-field in the starboard quarter and below the rotor. Pretest estimates indicated the peak acoustic radiation for this test configuration to be in this direction.

Another set of two microphones was mounted on a short sting from the RWTS placing them just under and to the side of the interaction position. They were approximately two blade chords from the leading edge of the blade at the 180 deg azimuth position (fig. 6). These microphones close to the interaction were included specifically to provide detailed information on the spatial evolution of the acoustic field. These data were collected to help validate “mid-field” calculations of computational aeroacoustics and Kirchhoff methods.

Bruel & Kjaer (B&K) 1/2-inch microphones with appropriate cathode followers and power supplies were used. For the wind-on data runs, standard B&K nose cones were installed.

Wind Tunnel Installation

The test section of the 80- by 120-Foot Wind Tunnel has approximately 6 inches of acoustic treatment in the floor and ceiling and 10 inches in the walls, yielding a cutoff frequency (for 90 percent absorption) of approximately 250 Hz. Although insufficient to accurately measure blade passage frequencies (60–70 Hz for this test), the treatment is adequate to measure the higher harmonics that are of most interest for BVI noise.

The RWTS/rotor system was installed on the horizontal centerline of the test section, with the rotor hub 15.65 feet above the tunnel floor.

The vortex generator (VG) was installed upstream of the RWTS with the trailing edge of the wing 48 inches upstream of the rotor blade tip at its 180 deg azimuth position. The height of the VG stand was such as to place the vortex for direct impact with the blade when the wing was at the mid-point of its extension limits. This allowed for placement of the vortex both above and below the blade. The VG vertical position was remotely set from the control room. The smoke generator for flow visualization of the vortex was mounted inside the vortex generator.

A long-range laser used to illuminate the vortex (seeded with smoke) and blade during the encounter was installed approximately 25 feet to the side of the RWTS. This laser was used to document the blade-vortex separation distance. The adjustable laser optics allowed positioning the laser sheet to intersect the blade and vortex just inboard of the tip. This cross section of the BVI event was recorded on a special high-speed, low-light video camera, mounted approximately 30 feet upstream of the RWTS. The camera shutter was slaved to the 1/rev trigger to capture the BVI event. A strobe, also slaved to the 1/rev trigger, illuminated the blade from below. A standard video camera, mounted below the rotor, verified that the vortex and blade were parallel during the encounter.

Test Procedures

Prior to the start of actual testing, some preliminary runs were carried out to check the acoustic reflection characteristics of the test arrangement and to calibrate the video system for quantitative measurements of the vortex-blade separation distance. Wind-on background noise measurements were performed after the completion of the data runs.

The testing proceeded in several stages. Since the vortex generator angle of attack had to be set manually, each stage corresponded to one value of this parameter and consisted of two sets of runs.

The first set was dedicated to flow visualization, while the second set was for blade pressure and acoustic data acquisition.

Flow visualization was used to determine the vertical position of the vortex generator that would yield the required vortex-blade separation distance. It was also used to ensure that the blade and the vortex were parallel during the encounter. During flow visualization, the pressure transducers were covered with tape to avoid contamination by the smoke particles. At each μ and M_{tip}, the smoke was released and the vortex generator moved to a series of vertical positions. Adjustments were made based on actual observed vortex-blade separation on the video monitor (the video display having been calibrated prior to the start of data runs). The position readings were noted for later duplication during the pressure data runs.

For the pressure data runs, the protective tape was removed from the transducers and each of the rotor and tunnel conditions was repeated while the vortex generator was positioned at the previously determined values. At each condition both blade pressure data and acoustic data were recorded. At some of the test conditions, the microphone traverse was moved to several streamwise positions to map out the acoustic field. This was not done for every test point due to time constraints.

This process was repeated for three vortex generator angle-of-attack settings. A summary of the test matrix is given in table 1.

Data Acquisition

Three data systems were used during this test. The Standard Wind Tunnel System (SWTS) recorded steady wind tunnel and rotor parameters.

A 32-channel, 16-bit digital data acquisition system acquired the 60 channels of blade pressure data in two sets. One transducer was duplicated between the two sets to check repeatability. The remaining channels were used to record two of the microphones. The incoming data were anti-alias filtered at 10 kHz. Individual channel gains were recorded as part of the data set. Thirty-two revolutions of data were recorded for each data point. Daily calibrations of the pressure transducers were performed by fitting a plexiglass tube over each blade, reducing the pressure inside the sealed chamber several psi, and recording the output voltage change from atmospheric as well as the indicated gauge pressure. “Zeros” (static nonrotating data) were acquired before rotor operation for each run.

Acoustic data were digitized on an Apple Macintosh-based, four-channel, 12-bit data system, in three sets, with some microphones duplicated between sets to verify consistency. One blade pressure transducer was also recorded on this system. The ALDAS data acquisition software (ref. 13) was used for data acquisition and processing. All incoming data were anti-alias filtered at 10 kHz. Individual channel gains could be set independently to maximize signal-to-noise ratio. Thirty revolutions of data were digitized for each data point. (Macintosh system memory was insufficient to digitize 32 revolutions of data.) In addition to this Macintosh-based system, 30 seconds of data were recorded on a digital tape recorder for archival purposes. Daily calibrations of the microphones were performed using a pistonphone.

The data acquisition on all data systems was triggered on the 1/rev synch signal, while the sampling clock was controlled by the 1024/rev TTL signal provided by the shaft encoder, resulting in a sampling rate of approximately 36,000 samples per second.

Data Processing

Blade Pressure Data

The 32 rotor revolutions of blade pressure data were ensemble averaged. It was verified that the data were highly repeatable and not degraded by the averaging process. The pressure data often contained zero shifts (DC offsets)—probably due to thermal effects which cause the transducer zeros to shift during the course of a run. These zero shifts cause errors in both the timewise and chordwise data plots. The time history data were greatly improved by digitally filtering out the four lowest blade passage harmonics. The resulting filtered plots are much more suitable for clearly discerning trends.

The zero shifts are more difficult to handle for displaying chordwise distributions of the data, fundamentally because the data originate from different transducers, not all of which exhibit large zero shifts of uniform magnitude. Chordwise pressure-coefficient distributions (where the pressure is nondimensionalized by the local dynamic pressure) on the advancing side of the rotor are almost always well behaved because the zero shift error is usually a small percentage of the dynamic pressure. On the retreating side, however, the dynamic pressure is much smaller and the nondimensionalization greatly exaggerates the effect of the zero shift error. The resulting chordwise distribution can be highly irregular. Therefore, to plot chordwise C_P distributions, the blade pressure zeros must be selectively adjusted so that the data display known spatial trends. (The chordwise pressure-coefficient distributions on the retreating side are well known because the overall lift is low and there are significant regions that lack blade-vortex interaction effects there. As was demonstrated in reference 12, when the zeros are adjusted to produce good pressure distributions on the retreating side, the resulting pressure coefficient plots are well behaved over the entire azimuth and compare well with predicted pressures.

Acoustic Data

The microphone data were processed using the ALDAS software (ref. 13). The data were converted to engineering units using sensitivities obtained from the pistonphone calibration performed prior to each day’s runs. Thirty revolutions of data were synchronously averaged based on the 1/rev trigger pulse, each sample of the average containing nominally 1024 points, representing one revolution of data. Due to a hardware/software operating limitation, in practice somewhat fewer than 1024 points were acquired for each revolution before sampling stopped and started again when the 1/rev trigger for the next revolution was detected. Thus a small percentage of data (typically approximately 5 points out of a total of 1024) at the end of each full revolution was missed. This did not have any significant effect on the results reported here.

As a check on the validity of this averaging procedure, the individual revolutions were compared to the calculated average to ensure that the BVI event was not smeared or smoothed by the averaging. In all cases, little or no evidence of smearing was observed.

Some preliminary attempts at isolating the BVI event by digitally filtering the data did not prove to be fruitful. Therefore, the presented data have not been filtered in any way (except for low-pass anti-aliasing filtering prior to digitization). In some cases the data were observed to contain DC shifts. These shifts were manually removed from the data by setting the mean waveform amplitude away from the BVI event to zero. (Since the raw data in counts did not show a DC offset, these DC shifts were thought to be a remnant of the unsteadiness introduced during the pistonphone calibration, resulting in a non-zero intercept value for the curve fit.)

DESCRIPTION OF DATA

Table 1 summarizes the operating conditions for which data were obtained. The main table indicates the combination of vortex "strength" and vertical position relative to the rotor. The key indicates the combination of rotor operating conditions that were tested. Preliminary data analysis indicated an error in the vertical position of the vortex for the $\alpha_V = +12°$ cases, which may have been due to a variety of reasons as discussed in detail in ref. 14. Table 1 reflects corrected z_V/c values for the latter cases. The majority of the data were obtained at rotational tip Mach numbers of 0.7 and 0.6 and rotor advance ratio of 0.2. Some additional data were obtained at low tip Mach numbers and lower advance ratios. This report presents data from the $M_{tip} = 0.7 / \mu = 0.2$ cases (marked ① on the "key" of table 1).

The data are presented in the Appendices in the form of averaged time histories of the acoustic and blade pressure data. There is also a CD-ROM which contain text files of the data. The disk and file formats are described in Appendix C.

REFERENCES

1. George, A. R.; and Chang, S. B.: Noise Due to Transonic Blade-Vortex Interactions. American Helicopter Society 39th Annual Forum, St. Louis, MO, May 1983.

2. Brentner, K. S.: Prediction of Helicopter Rotor Discrete Frequency Noise. NASA TM-87721, Oct. 1986.

3. Gallman, J. M.: The Validation and Application of a Rotor Acoustic Prediction Computer Program. Army Science Conference, Durham, NC, June 1990.

4. Xue, Y.; and Lyrintzis, A. S.: The Use of a Rotating Kirchoff Formulation for 3-D Transonic BVI Far-Field Noise. American Helicopter Society 49th Annual Forum, St. Louis, MO, May 1993.

5. Baeder, J. D.: The Computation and Analysis of Acoustic Waves In Transonic Airfoil-Vortex Interactions. Ph.D. Thesis, Stanford University, Sept. 1989.

6. Caradonna, F. X.; Laub, G. H.; and Tung, C.: An Experimental Investigation of the Parallel Blade-Vortex Interaction. 10th European Rotorcraft Forum, The Hague, Netherlands, Sept. 1984.

7. Caradonna, F. X.; Lautenschlager, J. L.; and Silva, M. J.: An Experimental Study of Rotor-Vortex Interactions. AIAA Paper 88-0045, AIAA 26th Aerospace Sciences Meeting, Reno, NV, Jan. 1988.

8. Caradonna, F. X.; Strawn, R. C.; and Bridgeman, J. O.: An Experimental and Computational Study of Rotor-Vortex Interactions. 14th European Rotorcraft Forum, Milano, Italy, Sept. 1988.

9. Obermeier, F.; and Schurman, O.: Experimental Investigation on 2D Blade-Vortex-Interaction Noise. AIAA Paper 93-4334, 15th AIAA Aeroacoustics Conference, Long Beach, CA, Oct. 1993.

10. Straus, J.; Renzoni, P.; and Mayle, R. E.: Airfoil Pressure Measurements During a Blade Vortex Interaction and a Comparison with Theory. AIAA J., vol. 28, no. 2, Feb. 1990.

11. McAlister, K. W.; and Takahashi, R. K.: NACA 0015 Wing Pressure and Trailing Vortex Measurements. NASA TP-3151, Nov. 1991.

12. Caradonna, F. X. et al.: A Review of Methods for the Prediction of BVI Noise. American Helicopter Society Technical Specialists’ Meeting for Rotorcraft Acoustics and Aerodynamics, Williamsburg, VA, Oct. 1997.

13. Watts, M. E.: ALDAS User’s Manual. NASA TM-102831, Apr. 1991.

14. Kitaplioglu, C.; Caradonna, F. X.; and Burley, C. L.: Parallel Blade-Vortex Interactions: An Experimental Study and Comparison with Computations. J. Am. Helicopter Soc., vol. 42, no. 3, July 1997.

Table 1. Summary of test parameters

alpha,v / zv/c	"-12deg"	"+6deg"	"+12deg"
0.25	① ② ⑥ ⑦	②	
0.125	① ②		① ② ⑥
0	① ② ⑤ ⑥ ⑦ ③ ④	① ②	① ②
-0.125	① ②		① ② ⑤ ⑥ ⑦ ③ ④
-0.25	① ② ⑥ ⑦	②	① ②
-0.4	① ② ⑥ ⑦	②	① ② ⑥ ⑦
-0.525			① ② ⑥ ⑦

KEY:

Mtip / μ	0.7	0.6	0.5	0.4	0.25
0.2	①	②	⑤	⑥	⑦
0.15		③			
0.1		④			

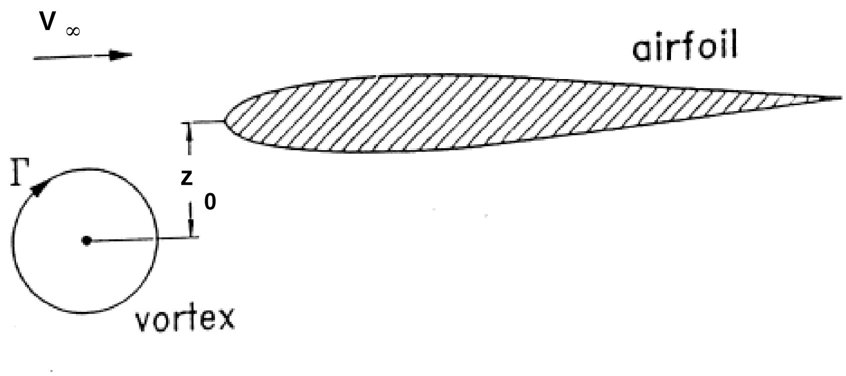

Figure 1. Simple 2-D model of parallel blade-vortex interaction.

Figure 2. BVI test in the Ames 80- by 120-Foot Wind Tunnel.

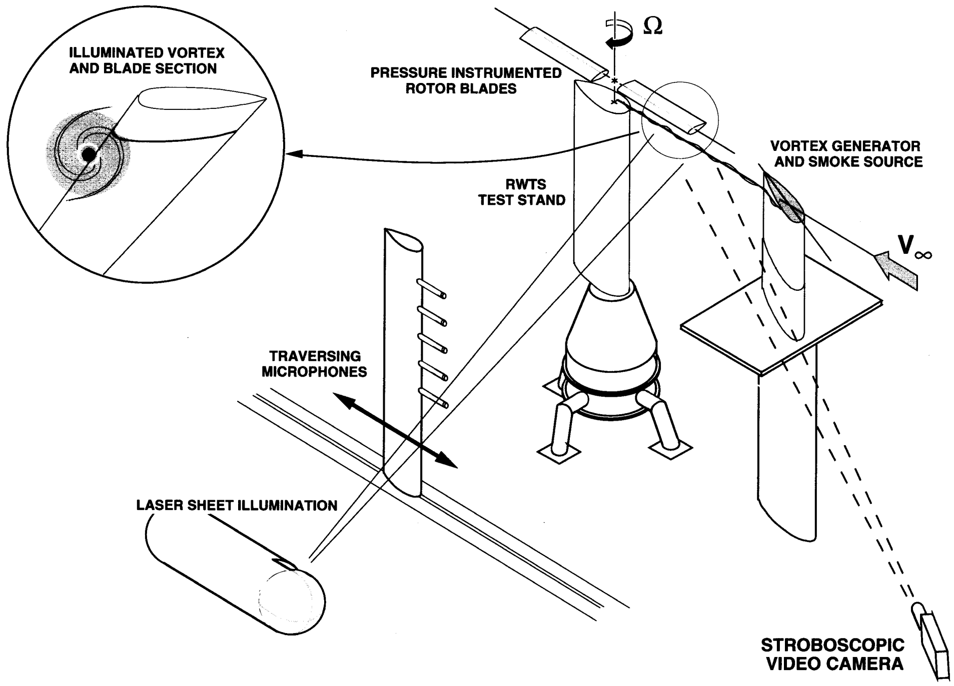

Figure 3. Schematic of BVI test in the 80- by 120-Foot Wind Tunnel.

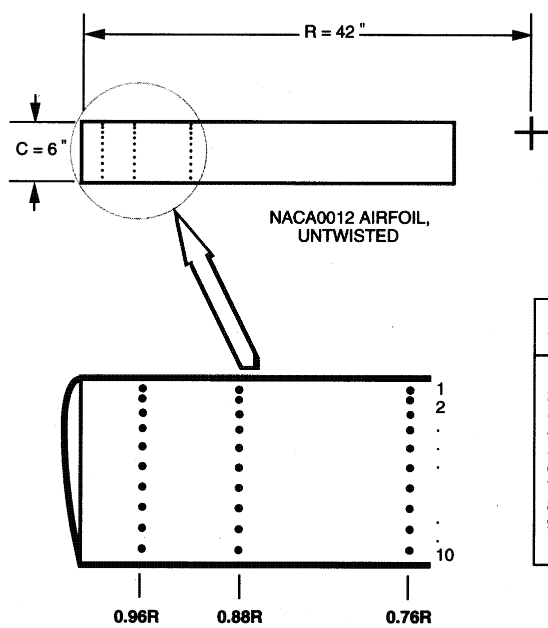

TRANSDUCER	CHORDWISE POSITION
1	0.02
2	0.11
3	0.20
4	0.31
5	0.40
6	0.48
7	0.56
8	0.64
9	0.72
10	0.83

Figure 4. Blade pressure transducer locations (not to scale). Identical locations for upper and lower surfaces.

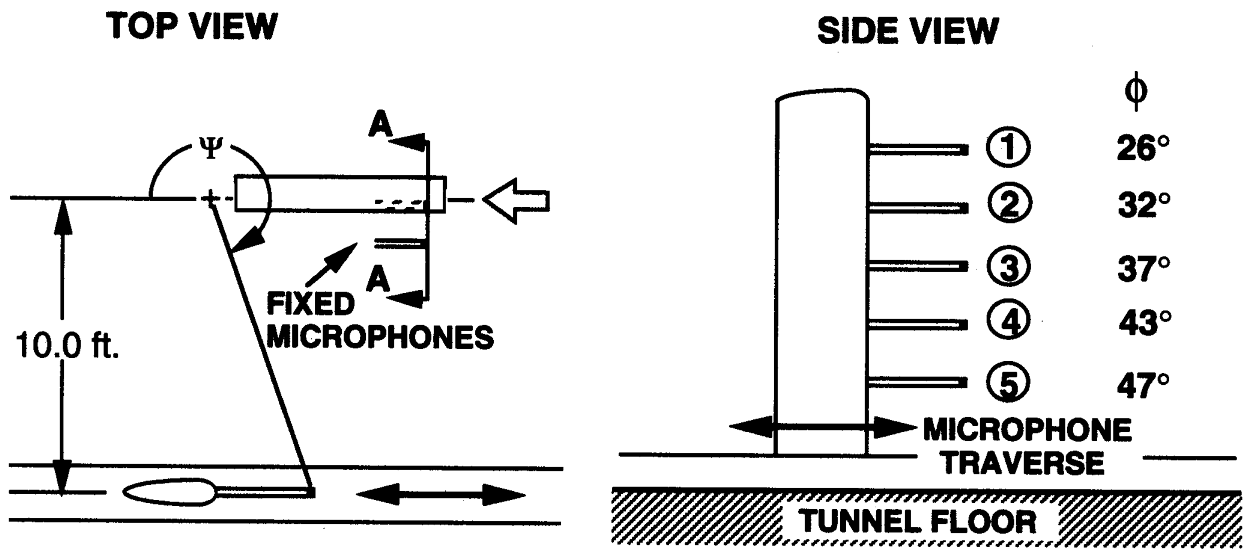

Figure 5. Far-field microphone positions (not to scale). Elevation angles are relative to the rotor plane.

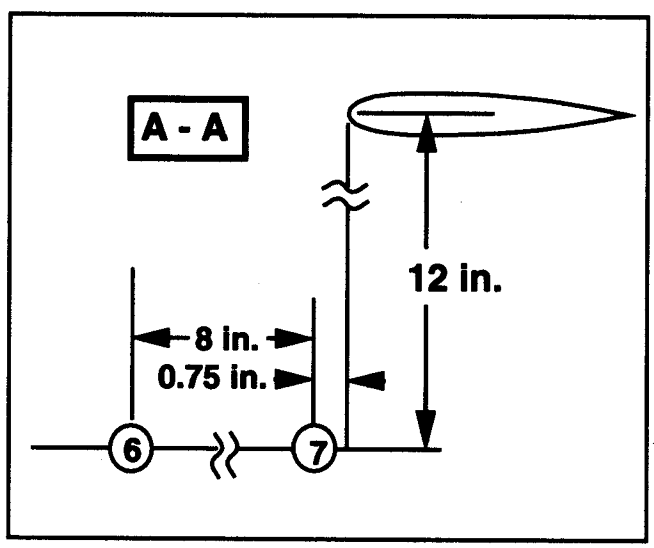

Figure 6. Near-field microphone positions; blade at Ψ=180° (not to scale).

APPENDICES

These appendices contain data from cases marked ① on the "key" of table 1, which were obtained at M_{tip} = 0.7 and μ = 0.2. The data are presented as follows:

Z_v/c	α_v = -12°	α_v = +12°
+0.25	A-1	B-1 (no data)
+0.125	A-2	B-2
0	A-3	B-3
-0.125	A-4	B-4
-0.25	A-5	B-5
-0.4	A-6	B-6 (no acoustic data)
-0.525	A-7 (no data)	B-7

Each appendix contains a list of the relevant test parameters, plots of the microphone time histories, and representative plots of Kulite time histories (mid-span, leading edge, top and bottom: Kulites 21 and 31 respectively).

Appendix C includes a CD-ROM containing text files of all the data, descriptions of the disk and file formats, and example printouts.

APPENDIX A-1

RUN 52 / POINT 7

α_V = -12°	z_V/c = +0.25
x_m = 0	RPM = 2131
M_{tip} = 0.715	θ_C = -0.15 °
μ = 0.198	C_T/σ = 0.0006
T_T = 56.8 °F	a_0 = 1111.87 ft/sec
p_S = -0.378 psi	ρ = 0.002363 slug/ft^3

RUN 50 / POINT 13

α_V = -12°	z_V/c = +0.25
x_m = 0	RPM = 2114
M_{tip} = 0.714	θ_C = -0.23°
μ = 0.198	C_T/σ = -0.0007
T_T = 49.5 °F	a_0 = 1103.98 ft/sec
p_S = -0.236 psi	ρ = 0.002407 slug/ft^3

RUN52/POINT07-MIC#2-TIME

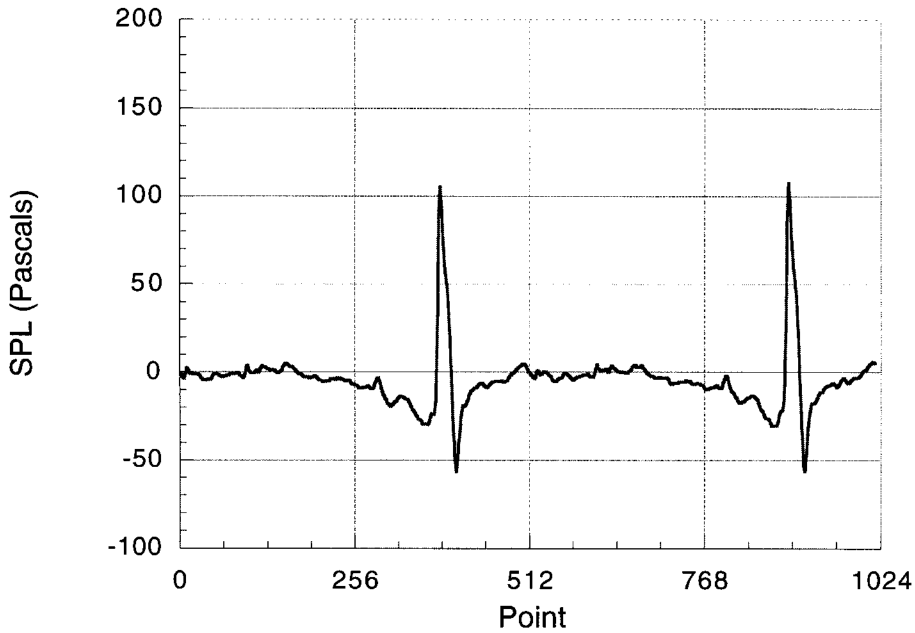

RUN52/POINT07-MIC#3-TIME

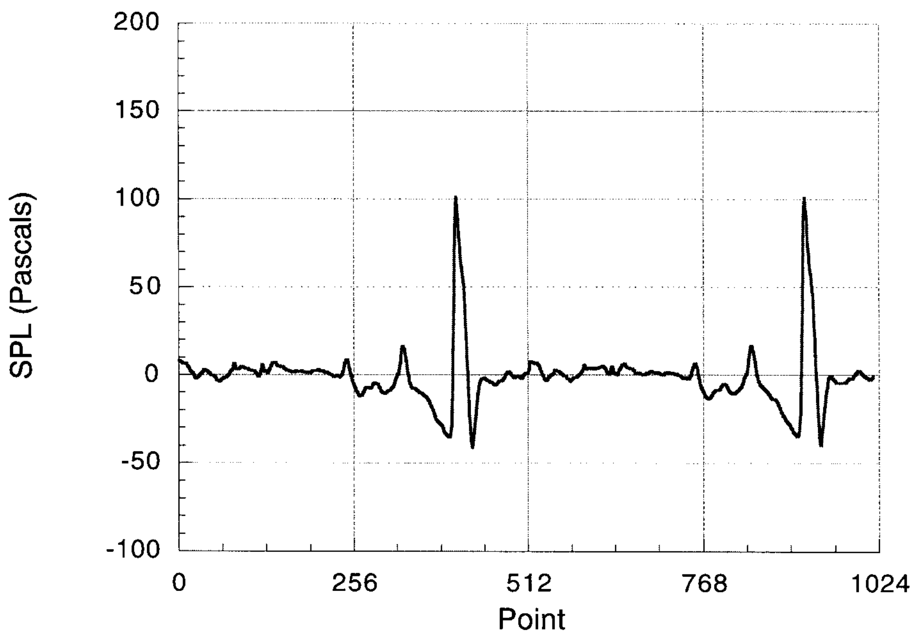

RUN52/POINT07-MIC#4-TIME

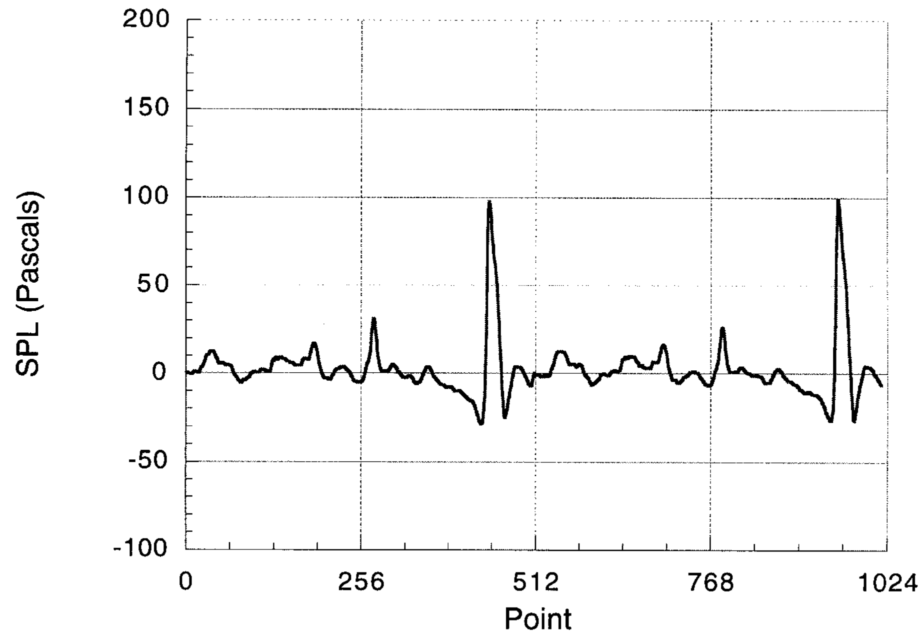

RUN52/POINT07-MIC#5-TIME

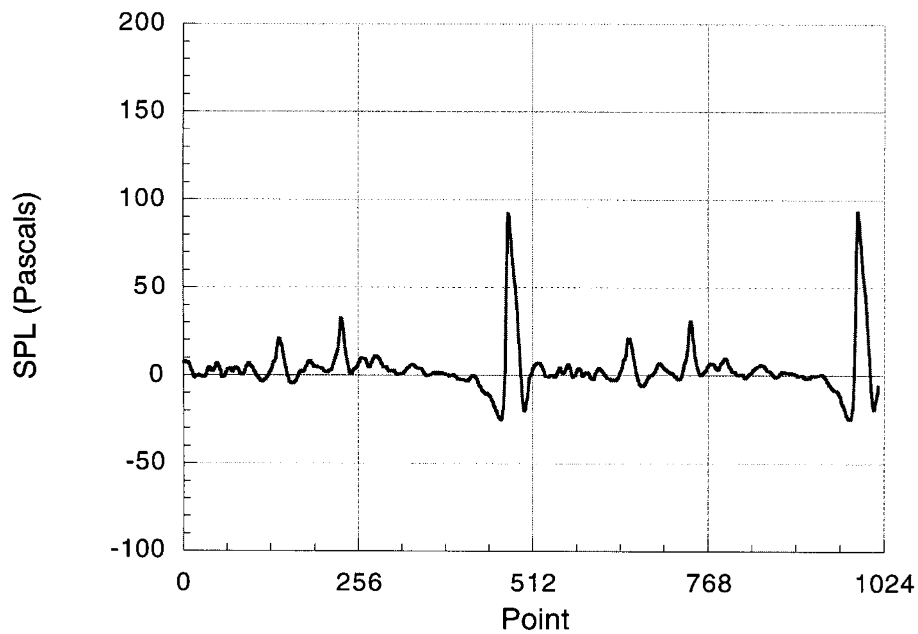

RUN52/POINT07-MIC#6-TIME

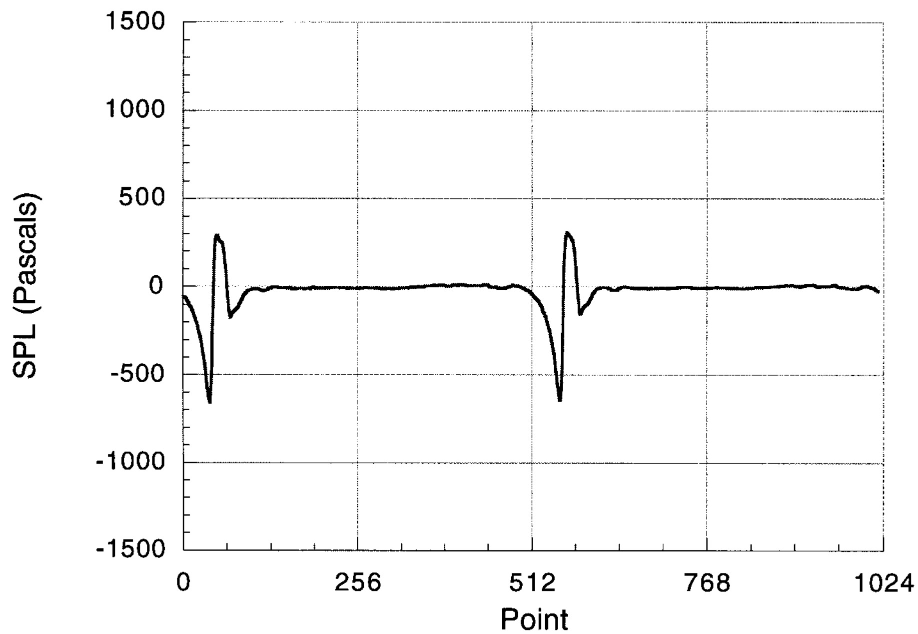

RUN52/POINT07-MIC#7-TIME

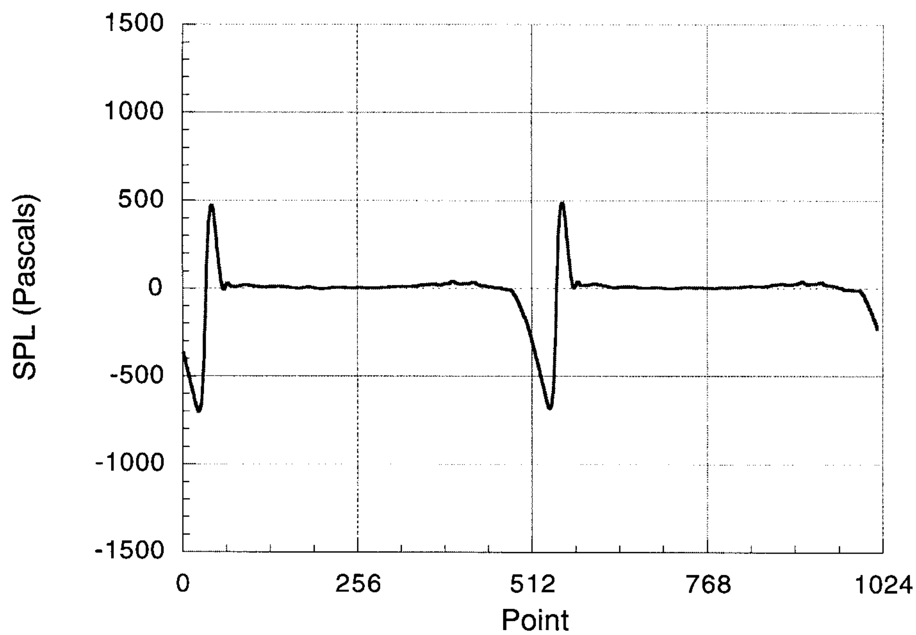

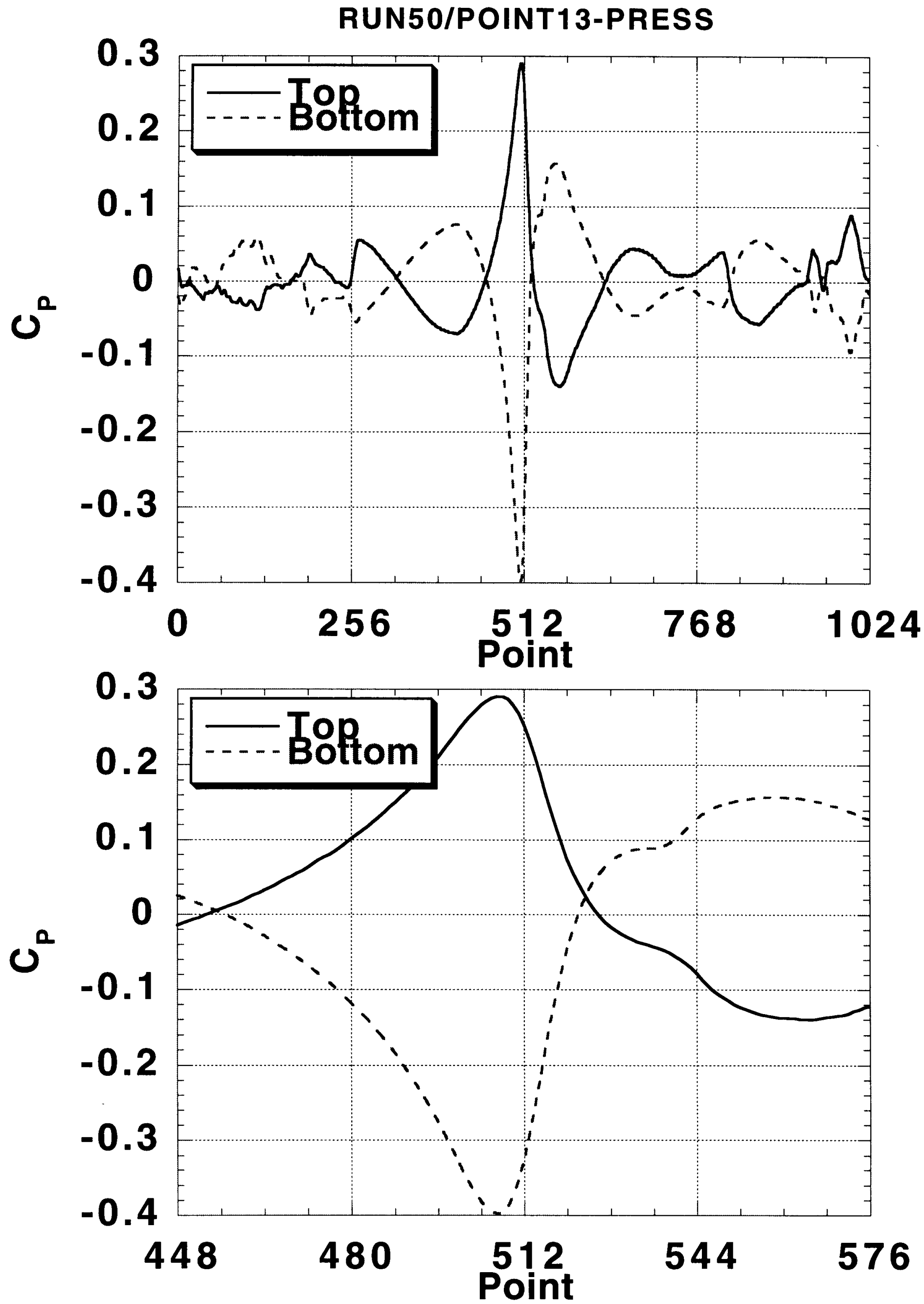
RUN50/POINT13-PRESS
Top
Bottom
0.3
0.2
0.1
0
-0.1
-0.2
-0.3
-0.4
C_P
0
256
512
768
1024
Point
Top
Bottom
C_P
448
480
512
544
576
Point

APPENDIX A-2

RUN 50 / POINT 12

α_V = -12°	z_V/c = +0.125
x_m = 0	RPM = 2112
M_{tip} = 0.712	θ_C = -0.21°
μ = 0.199	C_T/σ = -0.0004
T_T = 51.4 °F	a_0 = 1106.04 ft/sec
p_S = -0.236 psi	ρ = 0.002397 slug/ft^3

RUN50/POINT12-MIC#6-TIME

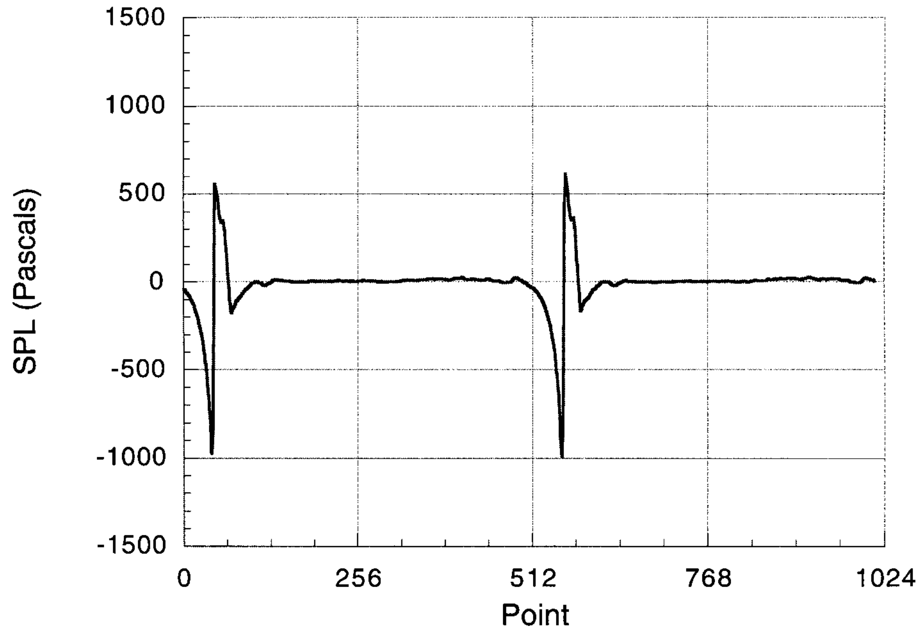

RUN50/POINT12-MIC#7-TIME

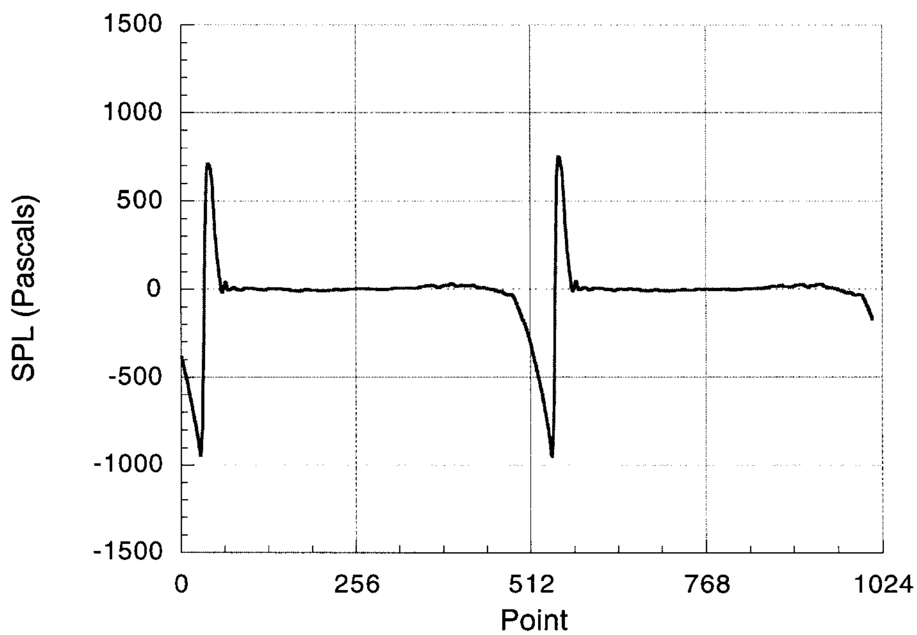

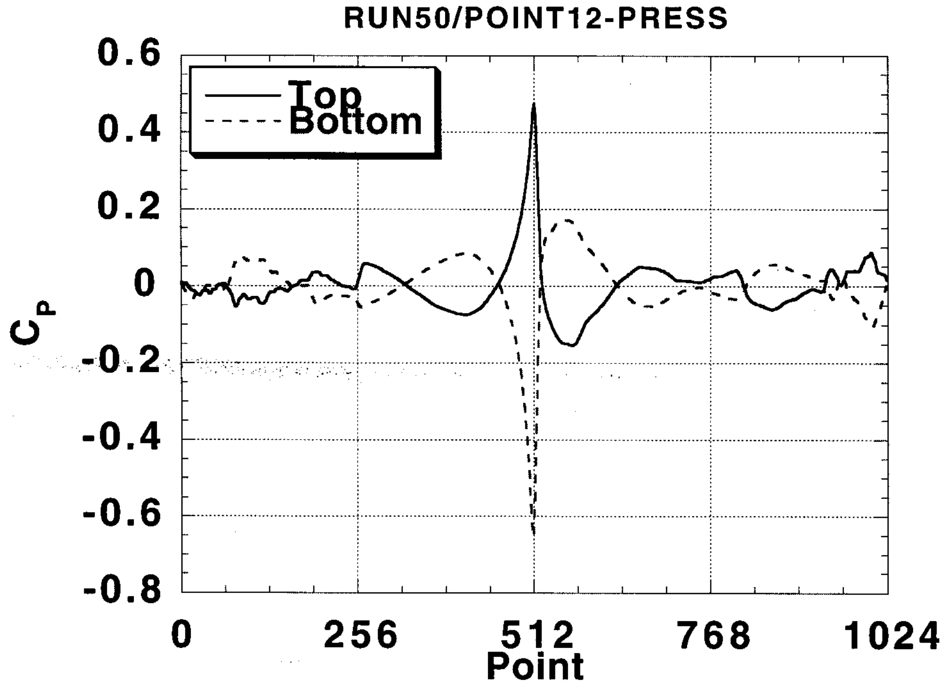
RUN50/POINT12-PRESS
Top
Bottom
C_P
0.6
0.4
0.2
0
-0.2
-0.4
-0.6
-0.8
0
256
512
768
1024
Point

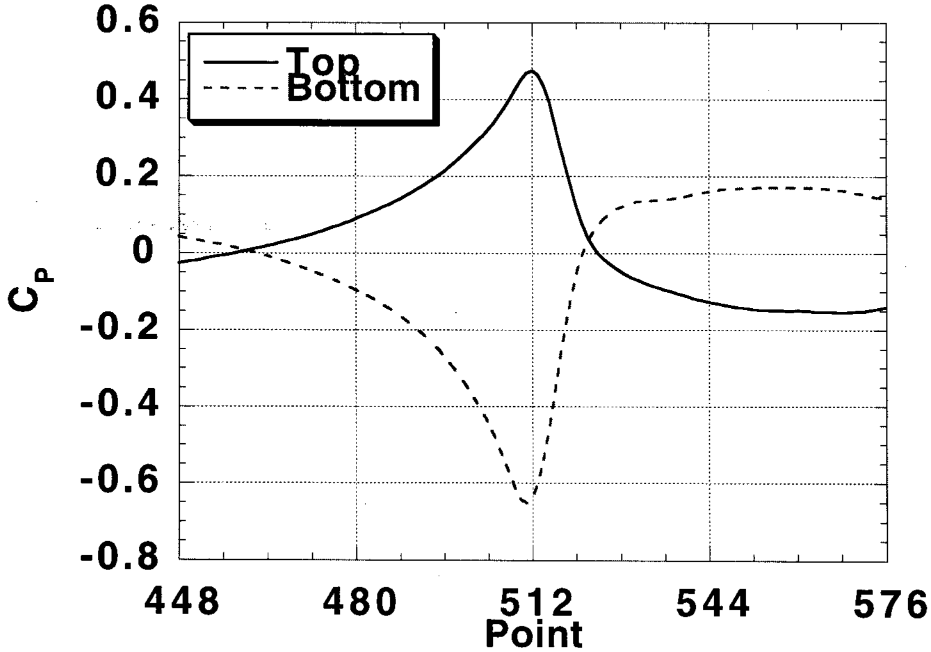
Top
Bottom
C_P
0.6
0.4
0.2
0
-0.2
-0.4
-0.6
-0.8
448
480
512
544
576
Point

APPENDIX A-3

RUN 52 / POINT 6

α_V = -12°	z_V/c = 0
x_m = 0	RPM = 2127
M_{tip} = 0.714	θ_C = -0.14°
μ = 0.198	C_T/σ = -0.0002
T_T = 55.9 °F	a_0 = 1110.91 ft/sec
p_S = -0.379 psi	ρ = 0.002368 slug/ft^3

RUN 50 / POINT 8

α_V = -12°	z_V/c = 0
x_m = 0	RPM = 2123
M_{tip} = 0.712	θ_C = -0.21°
μ = 0.198	C_T/σ = -0.0013
T_T = 51.9 °F	a_0 = 1105.59 ft/sec
p_S = -0.235 psi	ρ = 0.002395 slug/ft^3

RUN52/POINT06-MIC#2-TIME

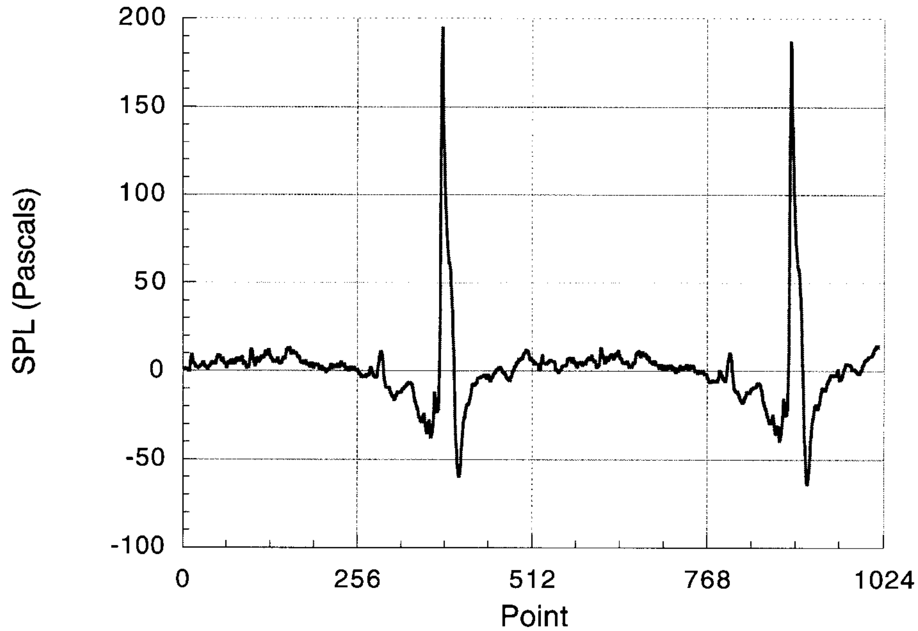

RUN52/POINT06-MIC#3-TIME

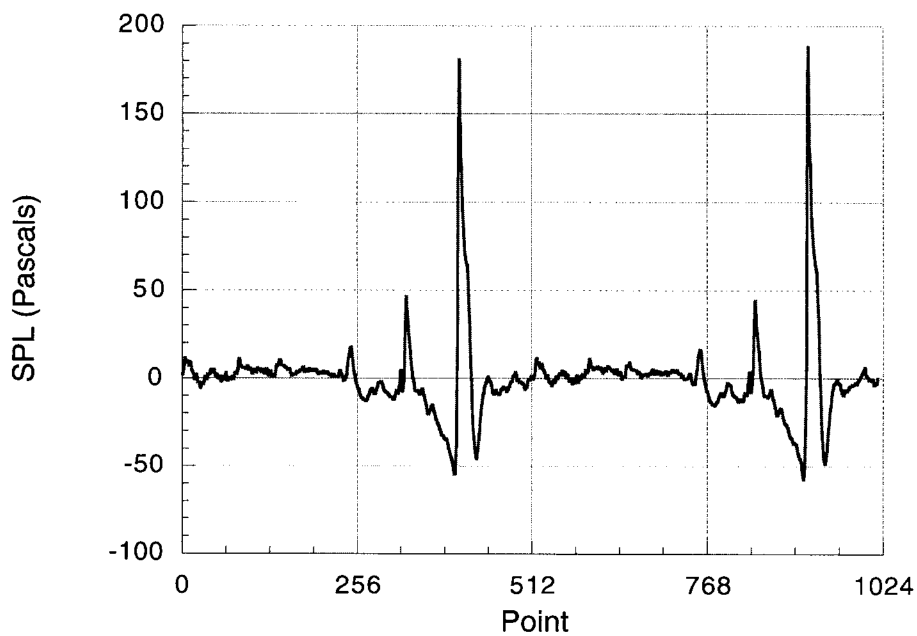

RUN52/POINT06-MIC#4-TIME

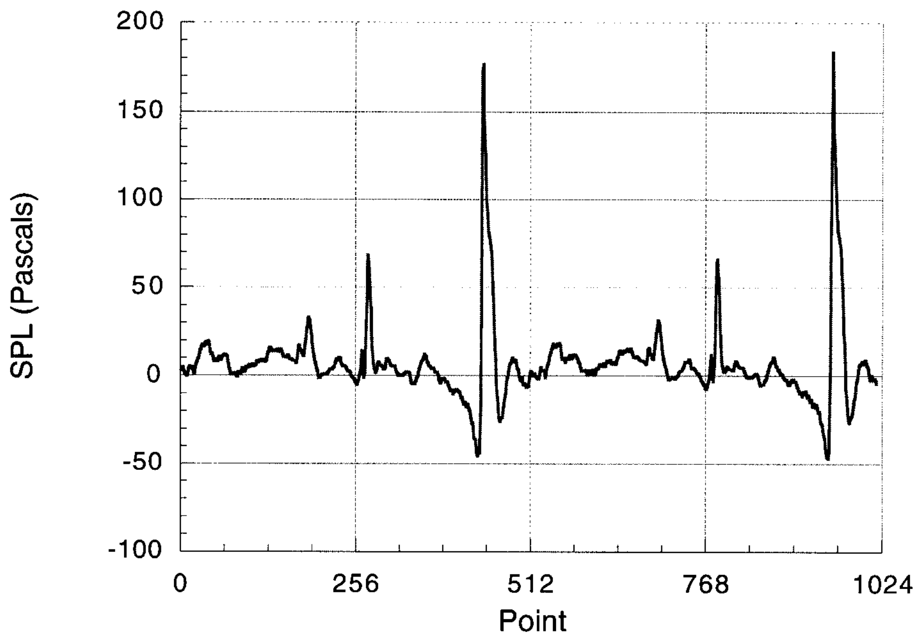

RUN52/POINT06-MIC#5-TIME

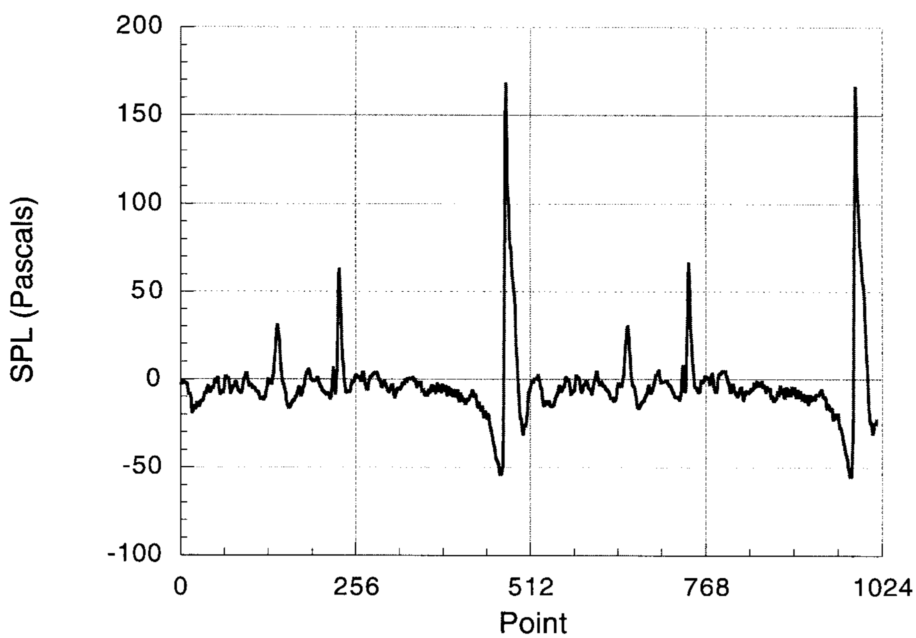

RUN52/POINT06-MIC#6-TIME

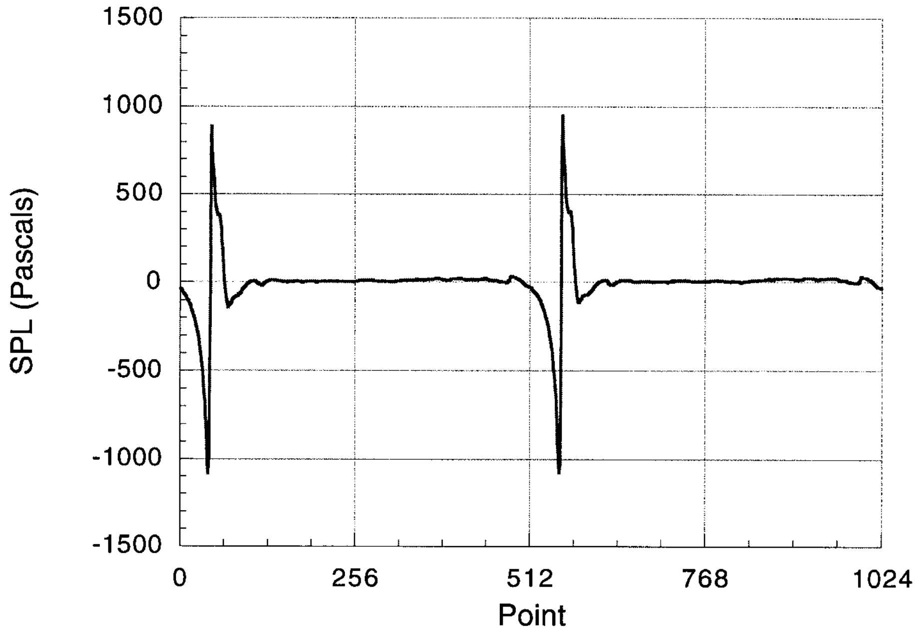

RUN52/POINT06-MIC#7-TIME

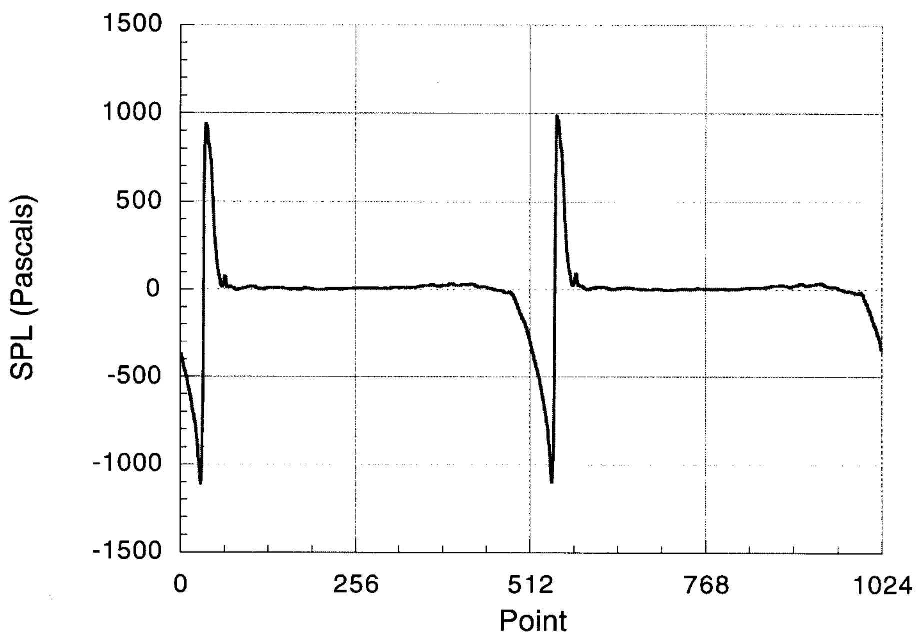

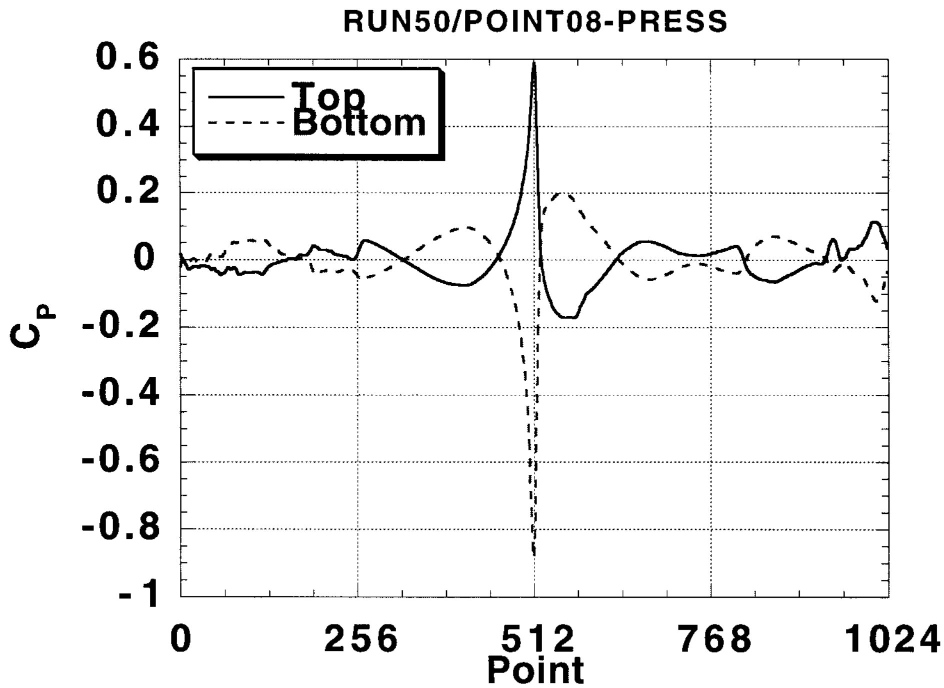
RUN50/POINT08-PRESS
Top
Bottom
C_p
Point
0.6
0.4
0.2
0
-0.2
-0.4
-0.6
-0.8
-1
0
256
512
768
1024

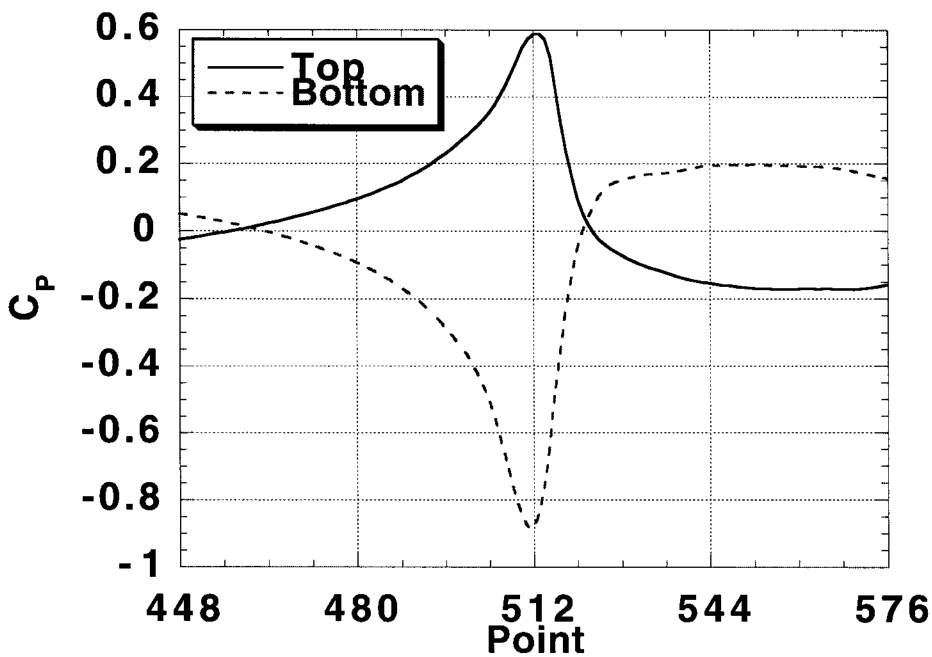
Top
Bottom
C_p
Point
0.6
0.4
0.2
0
-0.2
-0.4
-0.6
-0.8
-1
448
480
512
544
576

APPENDIX A-4

RUN 50 / POINT 7

α_V = -12°	z_V/c = -0.125
x_m = 0	RPM = 2113
M_{tip} = 0.714	θ_C = -0.21°
μ = 0.198	C_T/σ = -0.0022
T_T = 49.7 °F	a_0 = 1104.21 ft/sec
p_S = -0.235 psi	ρ = 0.002405 slug/ft^3

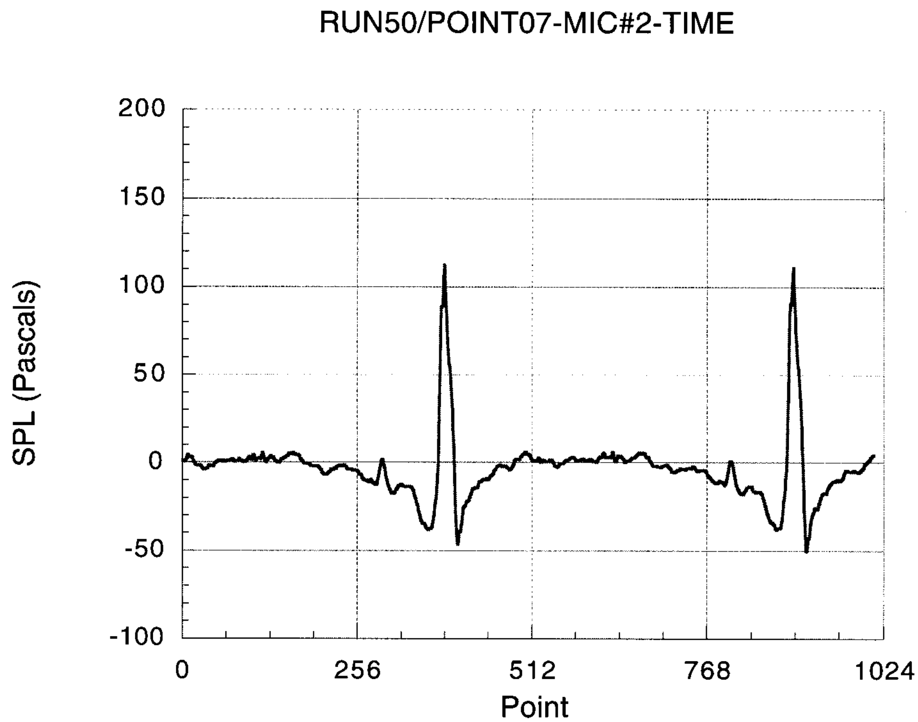
RUN50/POINT07-MIC#2-TIME
SPL (Pascals)
200
150
100
50
0
-50
-100
0
256
512
768
1024
Point

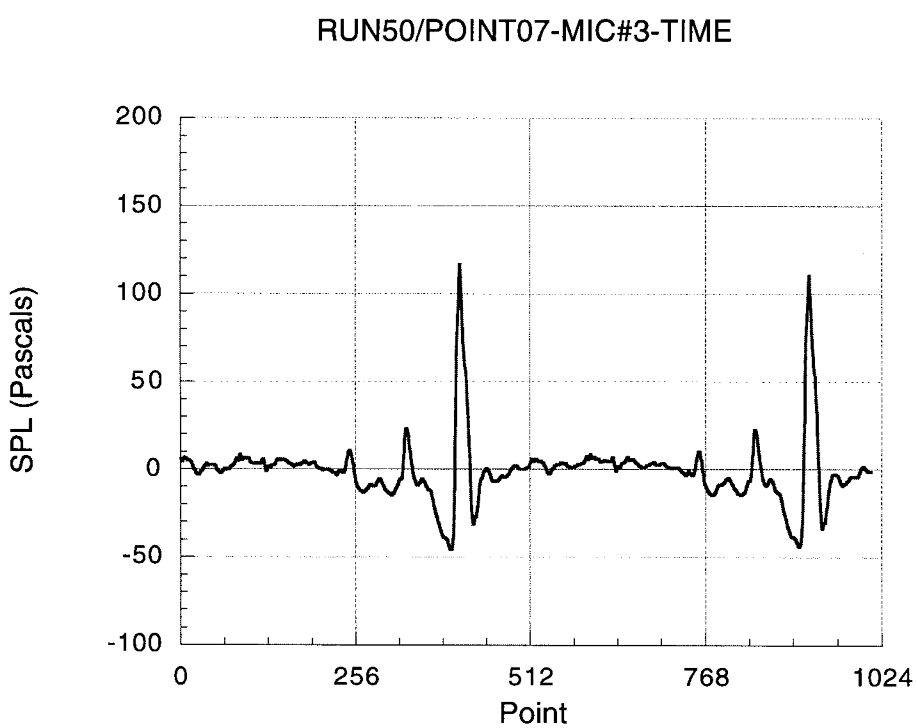
RUN50/POINT07-MIC#3-TIME
SPL (Pascals)
200
150
100
50
0
-50
-100
0
256
512
768
1024
Point

RUN50/POINT07-MIC#4-TIME

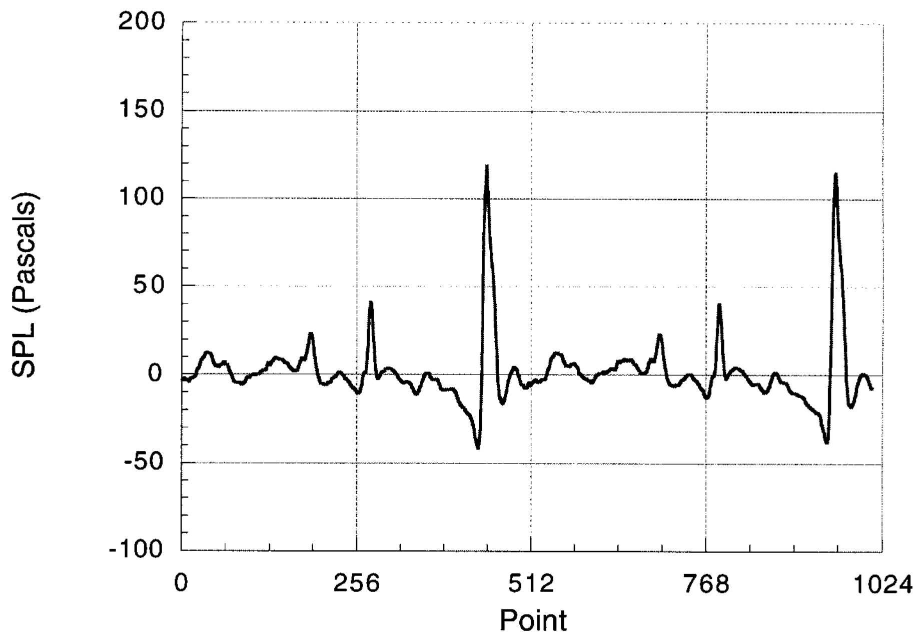

RUN50/POINT07-MIC#5-TIME

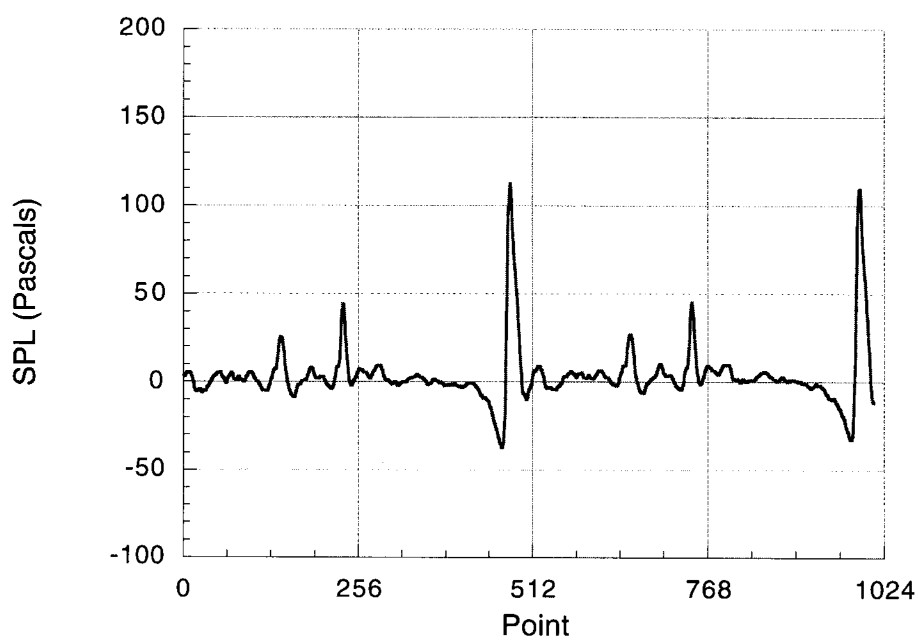

RUN50/POINT07-MIC#6-TIME

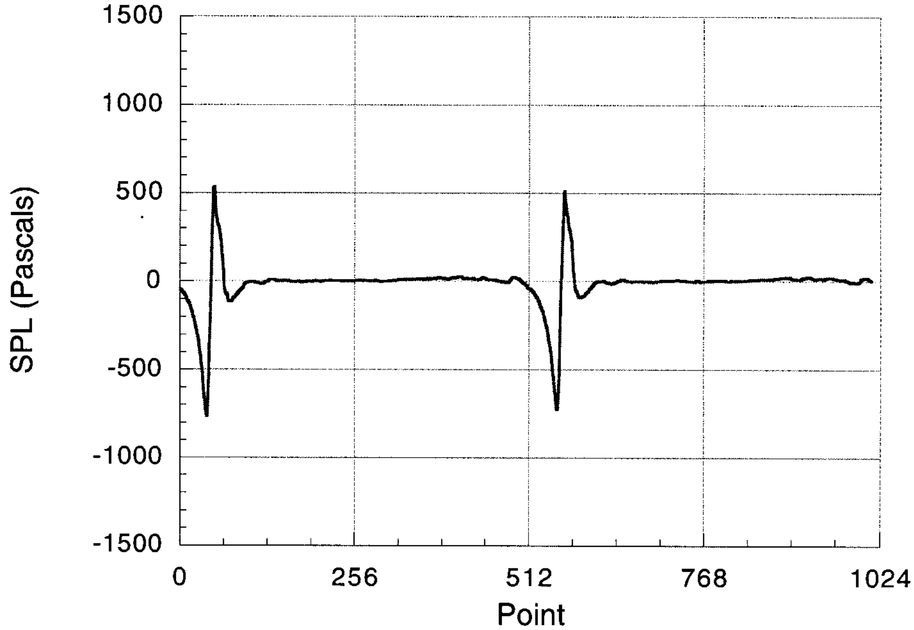

RUN50/POINT07-MIC#7-TIME

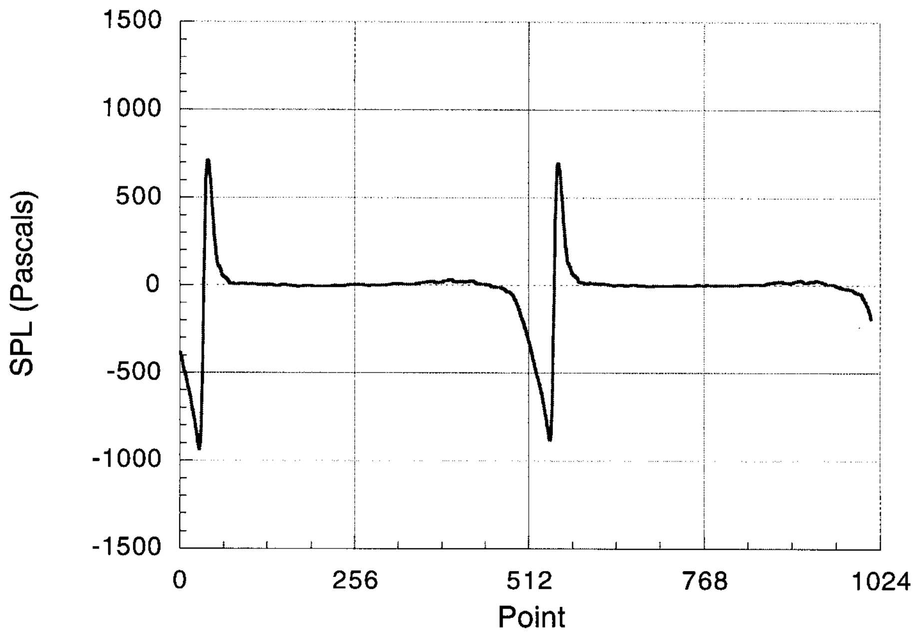

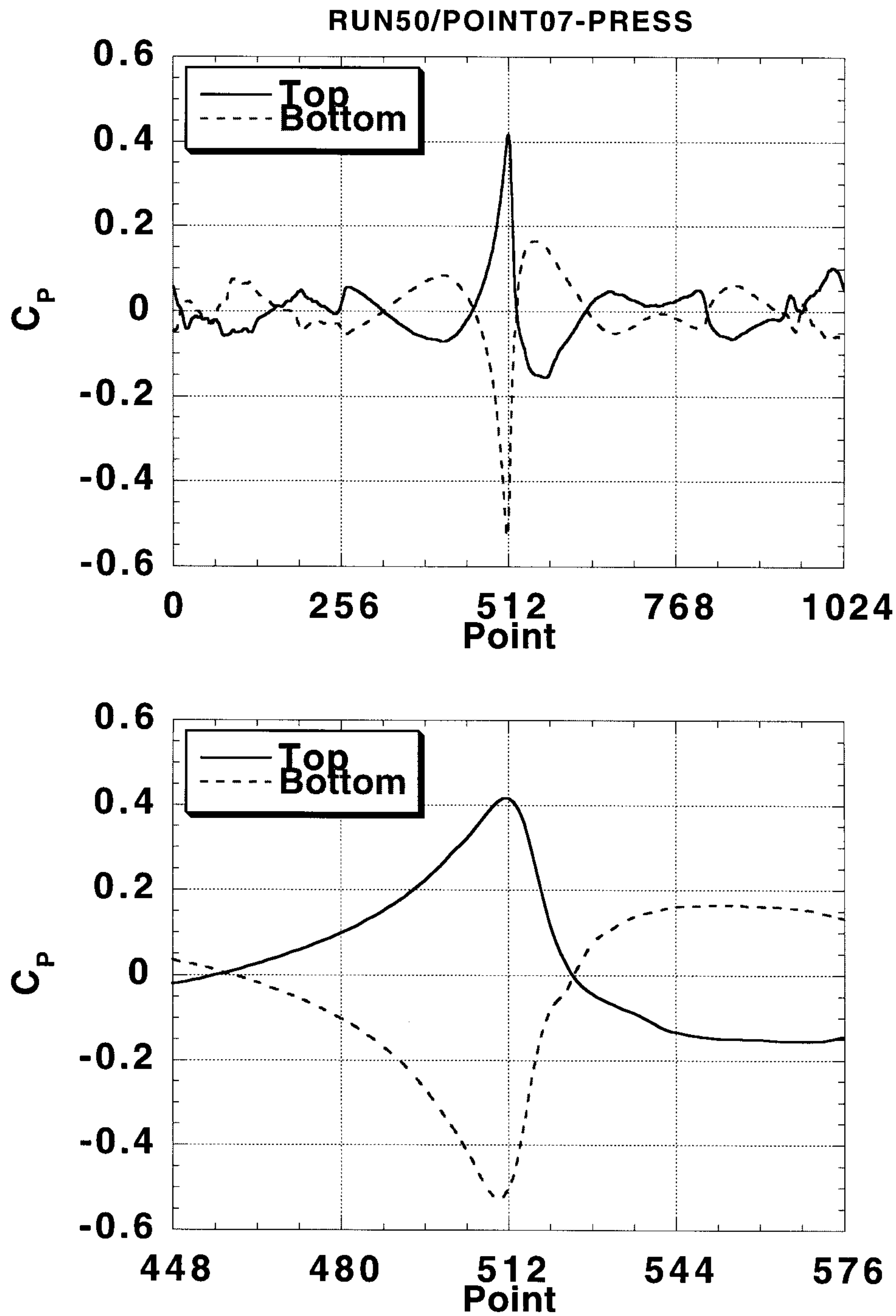
RUN50/POINT07-PRESS
Top
Bottom
C_P
0.6
0.4
0.2
0
-0.2
-0.4
-0.6
0
256
512
768
1024
Point
Top
Bottom
C_P
0.6
0.4
0.2
0
-0.2
-0.4
-0.6
448
480
512
544
576
Point

APPENDIX A-5

RUN 52 / POINT 8

α_V = -12°

z_V/c = -0.25

x_m = 0

RPM = 2129

M_{tip} = 0.715

θ_C = -0.15°

μ = 0.198

C_T/σ = 0.0007

T_T = 56.2 °F

a_0 = 1111.22 ft/sec

p_S = -0.378 psi

ρ = 0.002366 slug/ft^3

RUN 50 / POINT 6

α_V = -12°

z_V/c = -0.25

x_m = 0

RPM = 2117

M_{tip} = 0.714

θ_C = -0.23 °

μ = 0.198

C_T/σ = 0.0017

T_T = 52.1 °F

a_0 = 1105.81 ft/sec

p_S = -0.235 psi

ρ = 0.002393 slug/ft^3

RUN52/POINT08-MIC#2-TIME

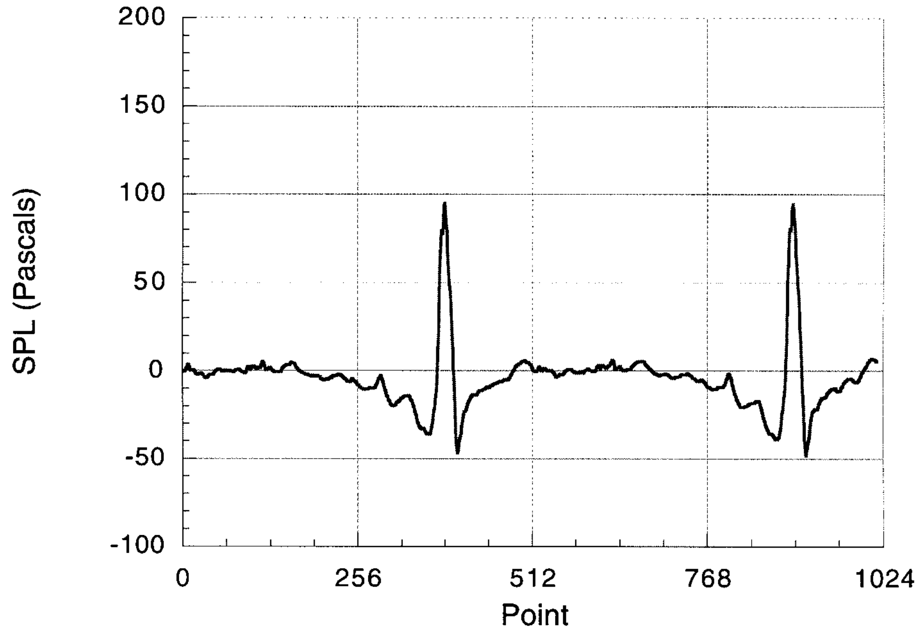

RUN52/POINT08-MIC#3-TIME

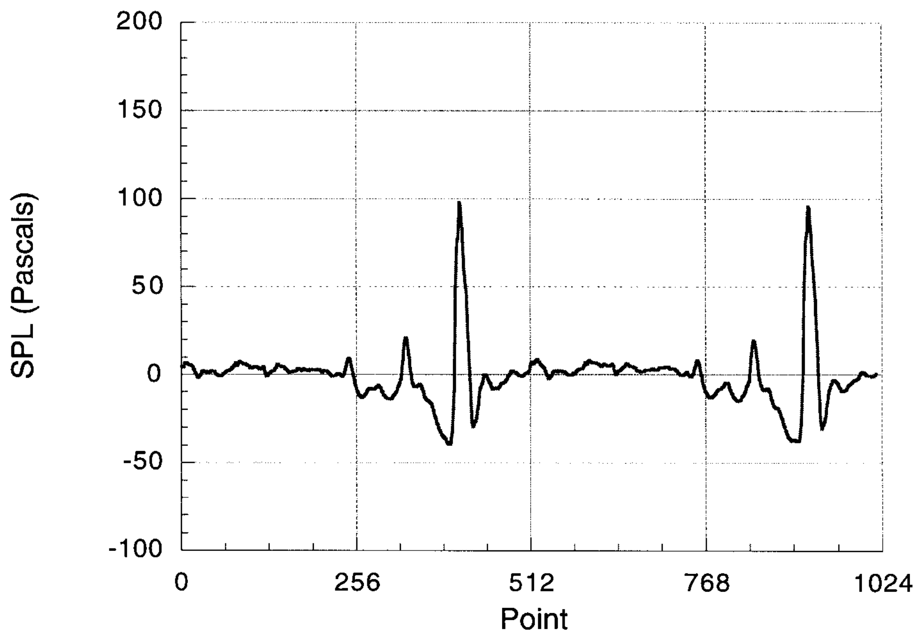

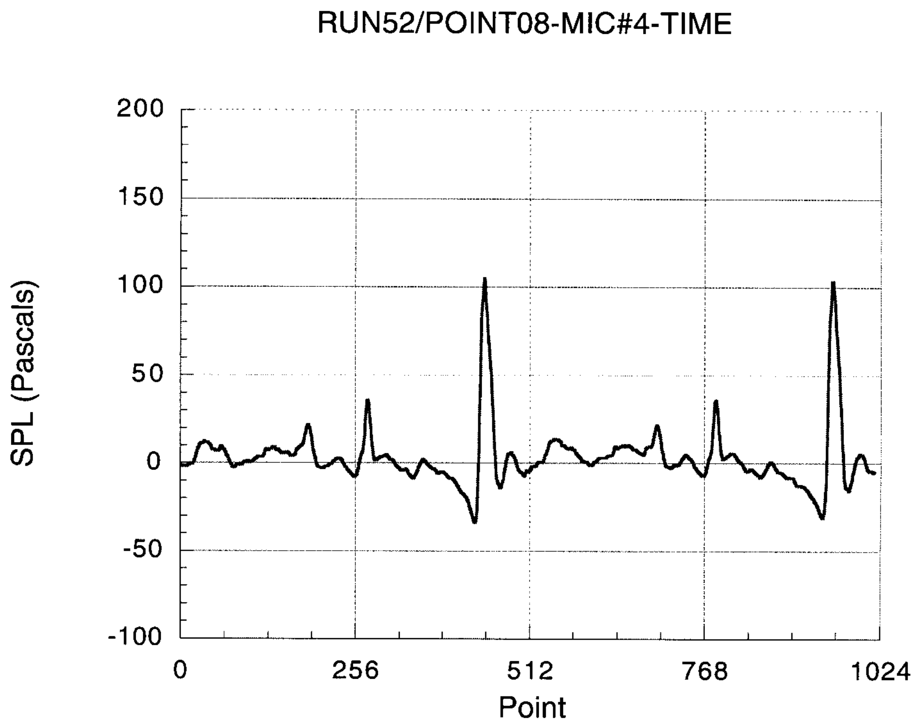
RUN52/POINT08-MIC#4-TIME
200
150
100
50
0
-50
-100
SPL (Pascals)
0
256
512
768
1024
Point

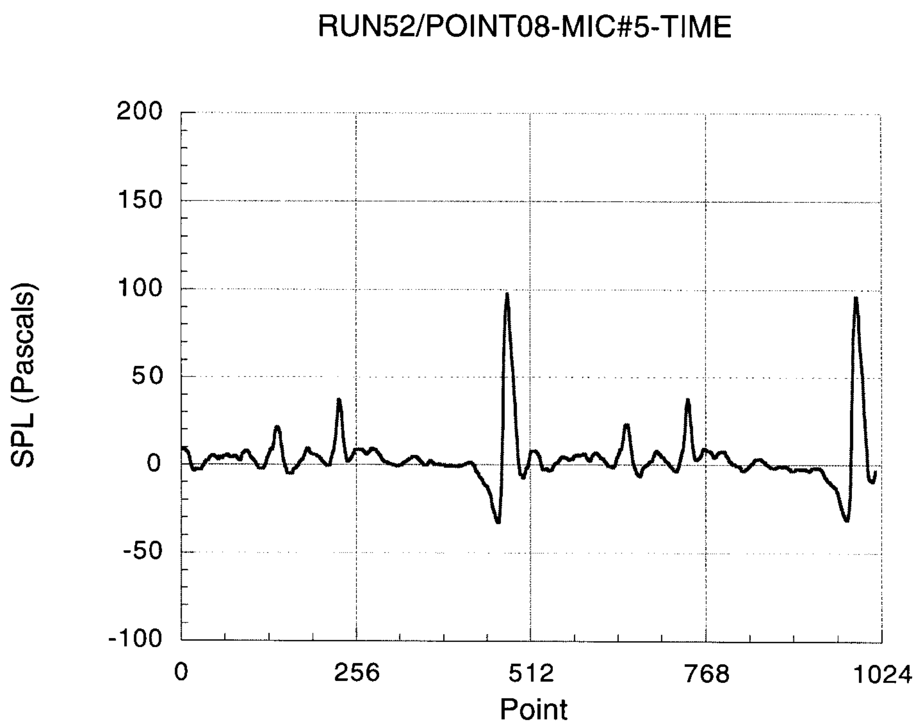
RUN52/POINT08-MIC#5-TIME
200
150
100
50
0
-50
-100
SPL (Pascals)
0
256
512
768
1024
Point

RUN52/POINT08-MIC#6-TIME

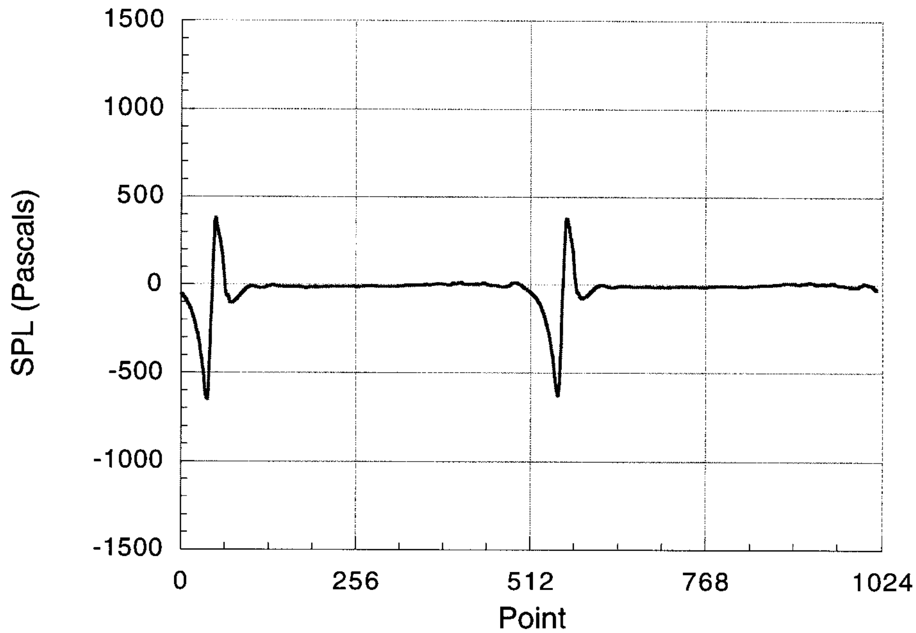

RUN52/POINT08-MIC#7-TIME

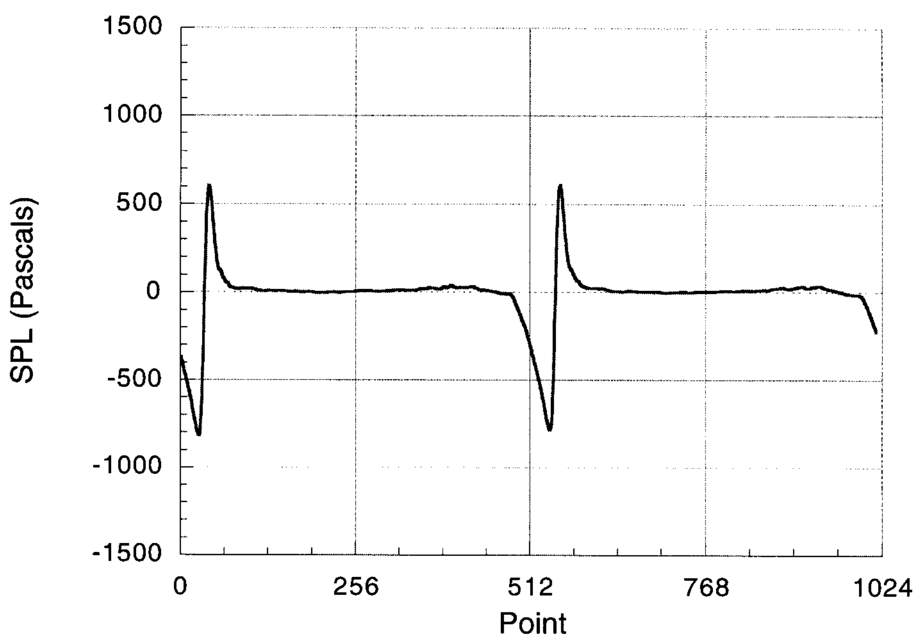

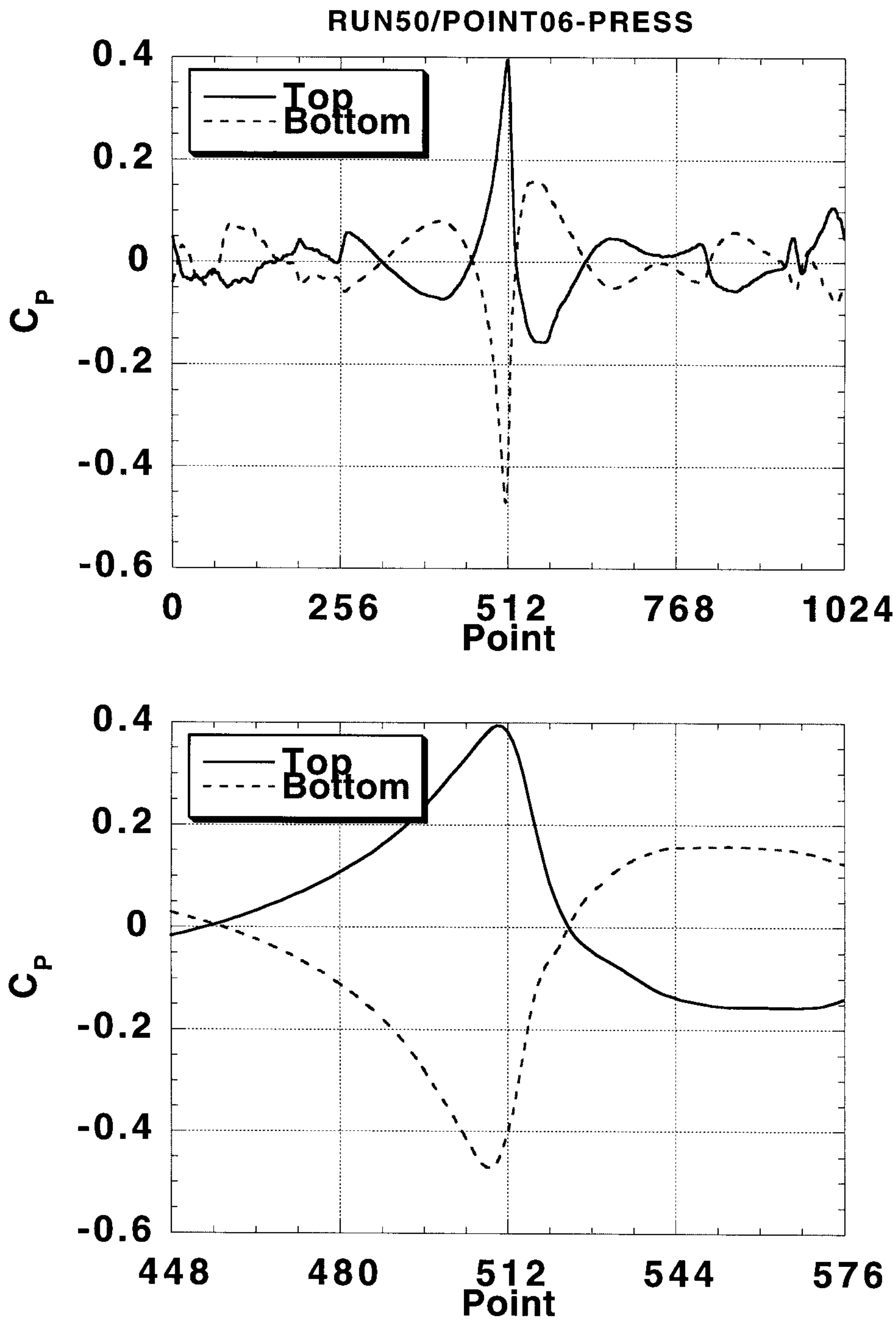
RUN50/POINT06-PRESS
Top
Bottom
0.4
0.2
0
-0.2
-0.4
-0.6
C_P
0
256
512
768
1024
Point
Top
Bottom
0.4
0.2
0
-0.2
-0.4
-0.6
C_P
448
480
512
544
576
Point

APPENDIX A-6

RUN 50 / POINT 5

α_V = -12°	z_V/c = -0.4
x_m = 0	RPM = 2118
M_{tip} = 0.713	θ_C = -0.24°
μ = 0.198	C_T/σ = -0.0011
T_T = 52.7 °F	a_0 = 1107.46 ft/sec
p_S = -0.235 psi	ρ = 0.002390 slug/ft^3

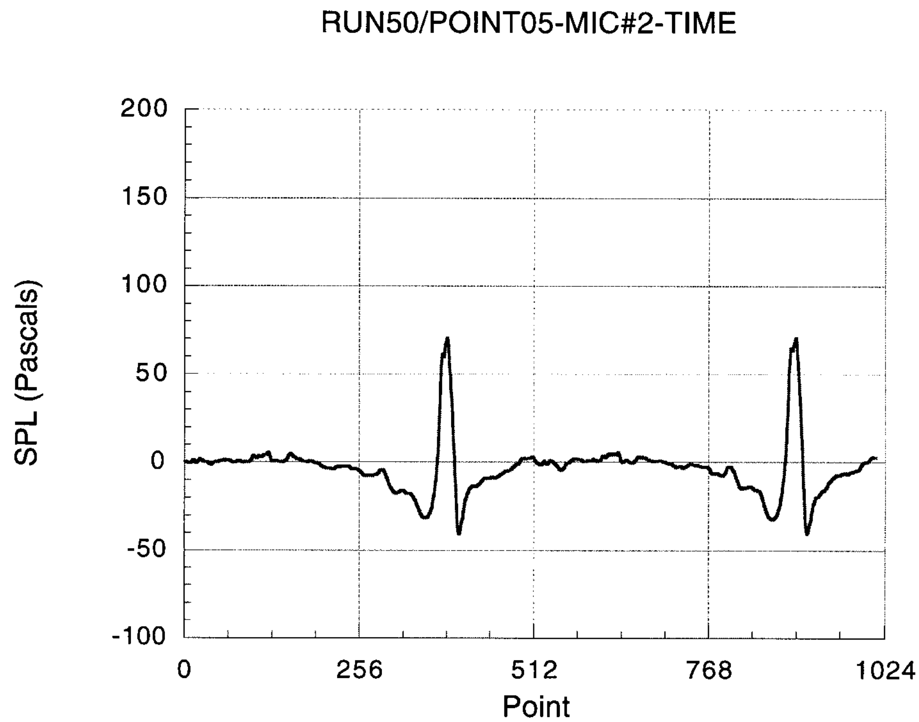
RUN50/POINT05-MIC#2-TIME
SPL (Pascals)
200
150
100
50
0
-50
-100
0
256
512
768
1024
Point

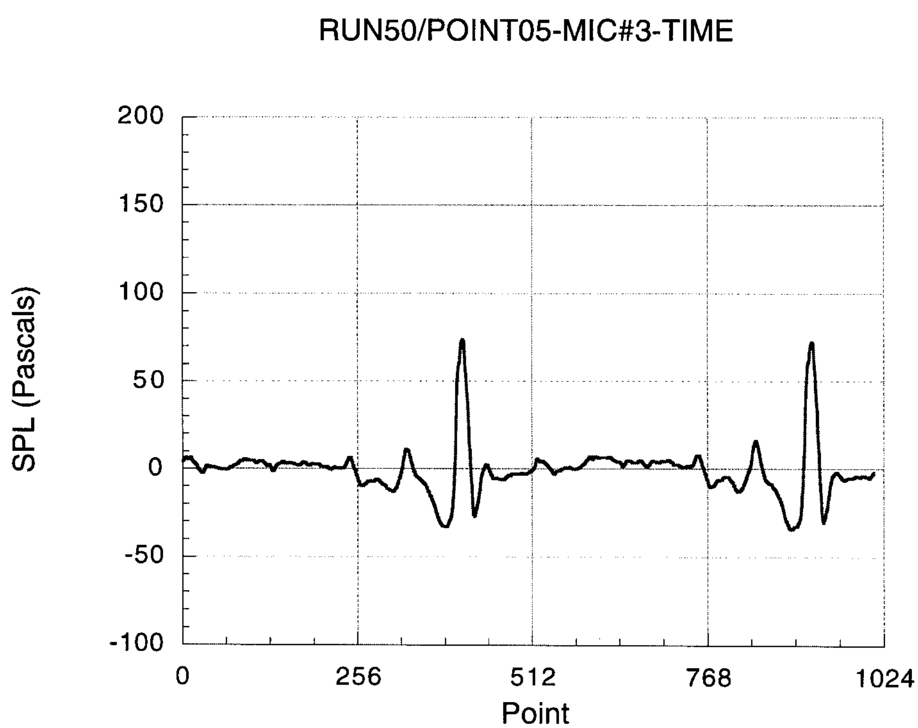
RUN50/POINT05-MIC#3-TIME
SPL (Pascals)
200
150
100
50
0
-50
-100
0
256
512
768
1024
Point

RUN50/POINT05-MIC#4-TIME

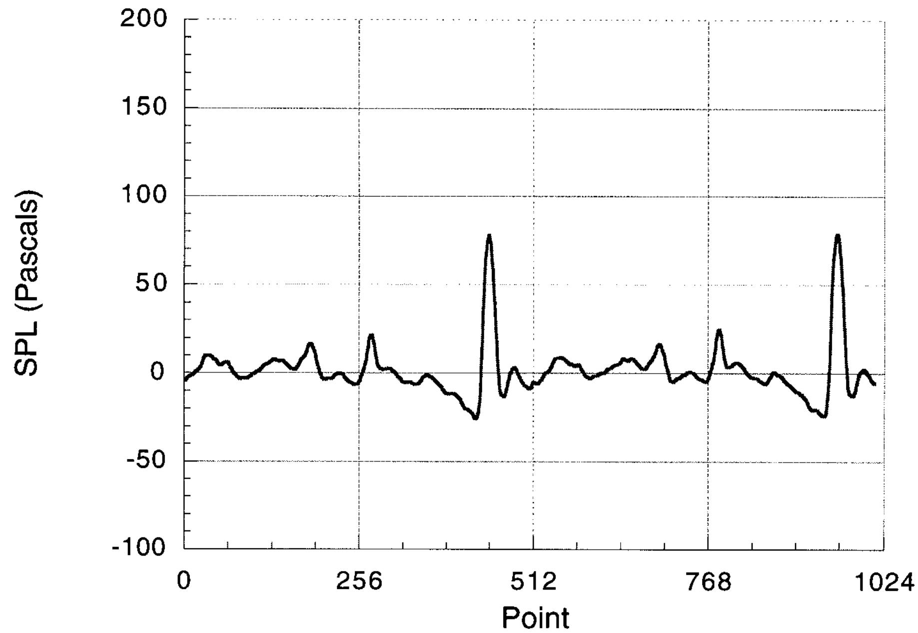

RUN50/POINT05-MIC#5-TIME

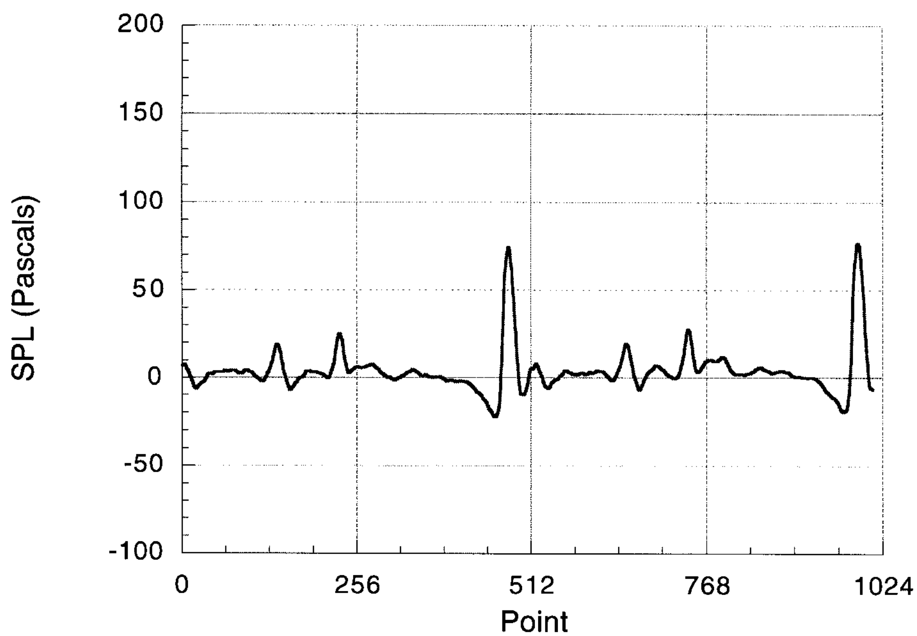

RUN50/POINT05-MIC#6-TIME

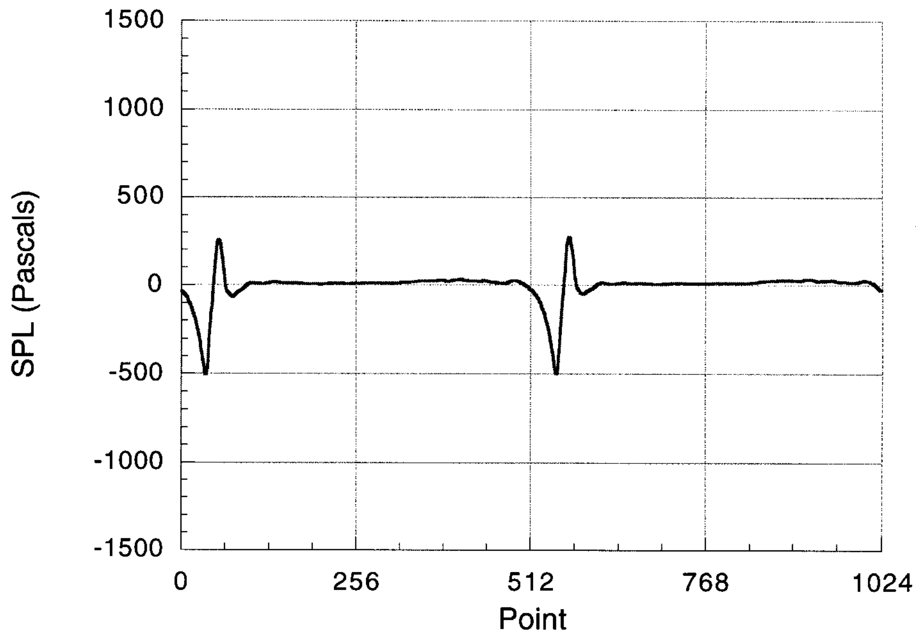

RUN50/POINT05-MIC#7-TIME

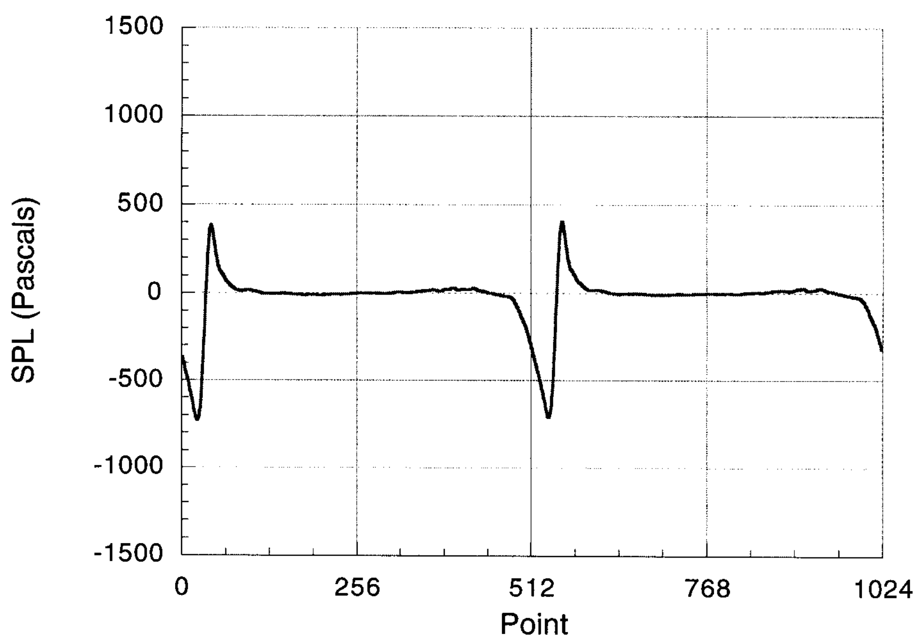

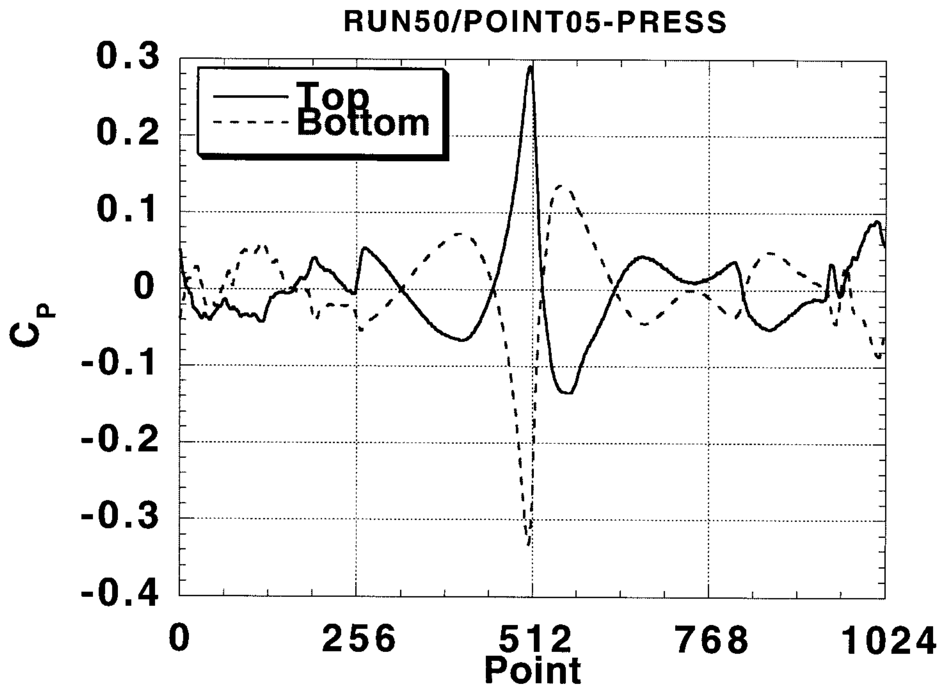
RUN50/POINT05-PRESS
Top
Bottom
0.3
0.2
0.1
0
-0.1
-0.2
-0.3
-0.4
C_P
0
256
512
768
1024
Point

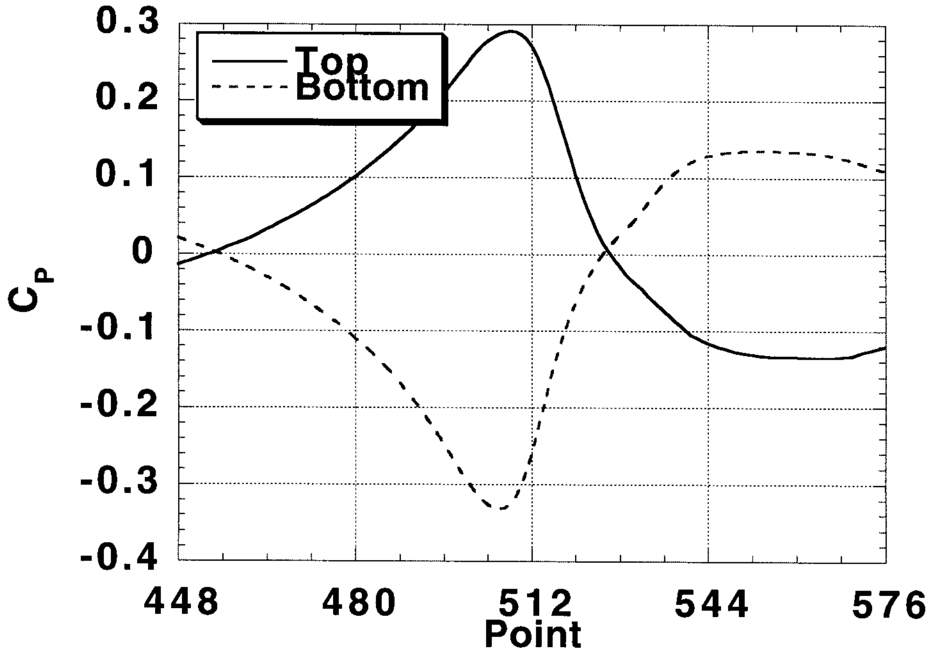
Top
Bottom
0.3
0.2
0.1
0
-0.1
-0.2
-0.3
-0.4
C_P
448
480
512
544
576
Point

APPENDIX A-7

$\alpha_V = -12°$ $z_V/c = -0.525$

NO DATA

APPENDIX B-1

$\alpha_V = +12°$ $z_V/c = +0.25$

NO DATA

APPENDIX B-2

RUN 49 / POINT 10

α_V = +12°

z_V/c = +0.125

x_m = 0

RPM = 2136

M_{tip} = 0.716

θ_C = -0.32°

μ = 0.198

C_T/σ = -0.0045

T_T = 57.8 °F

a_0 = 1112.94 ft/sec

p_S = -0.237 psi

ρ = 0.002364 slug/ft^3

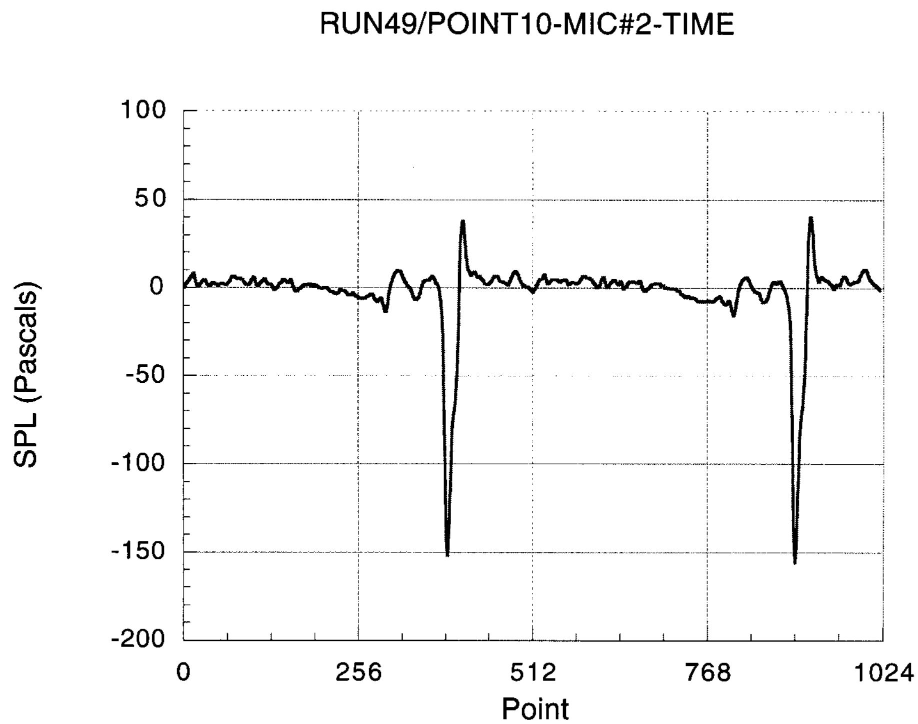

RUN49/POINT10-MIC#2-TIME
SPL (Pascals)
100
50
0
-50
-100
-150
-200
0
256
512
768
1024
Point

RUN49/POINT10-MIC#4-TIME

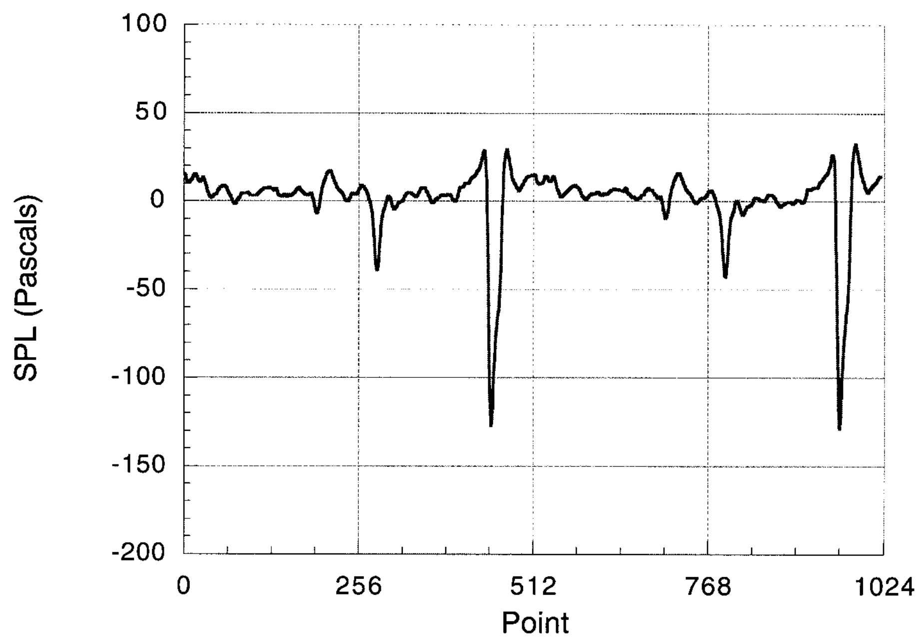

RUN49/POINT10-MIC#5-TIME

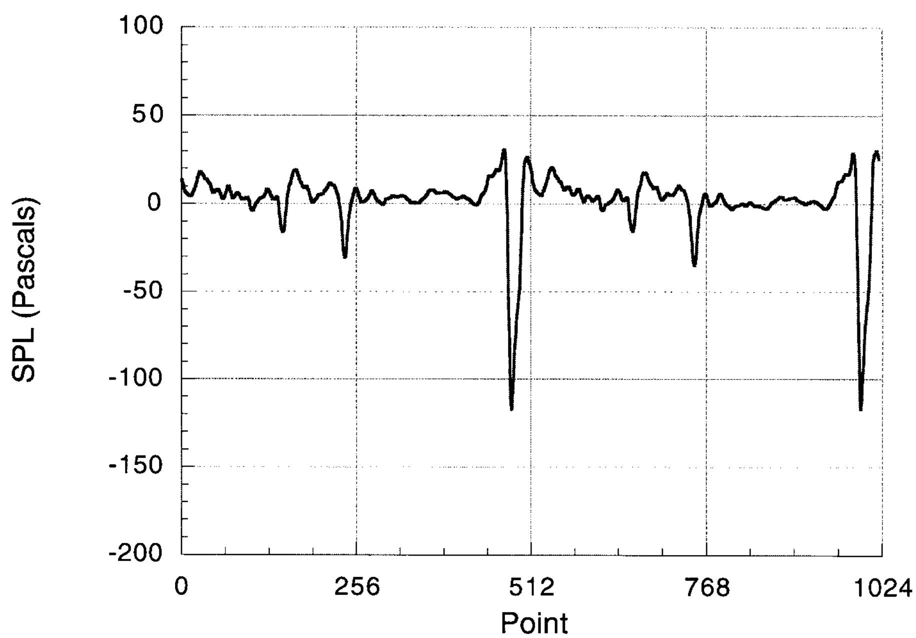

RUN49/POINT10-MIC#6-TIME

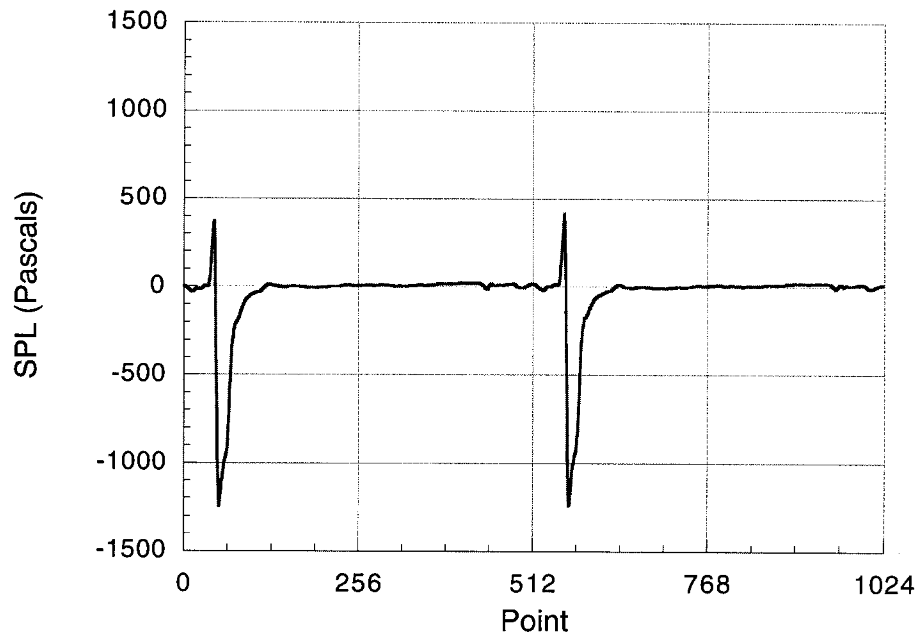

RUN49/POINT10-MIC#7-TIME

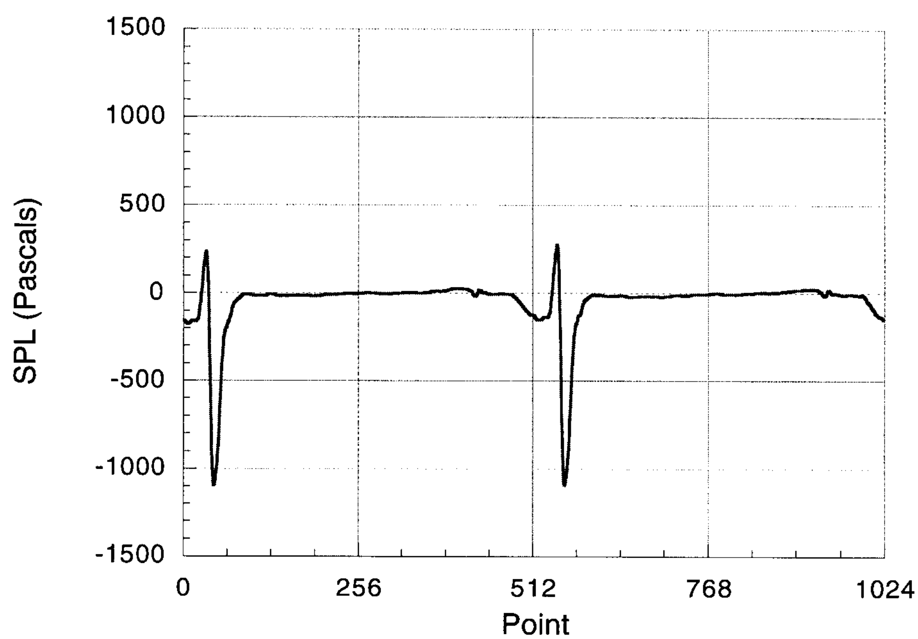

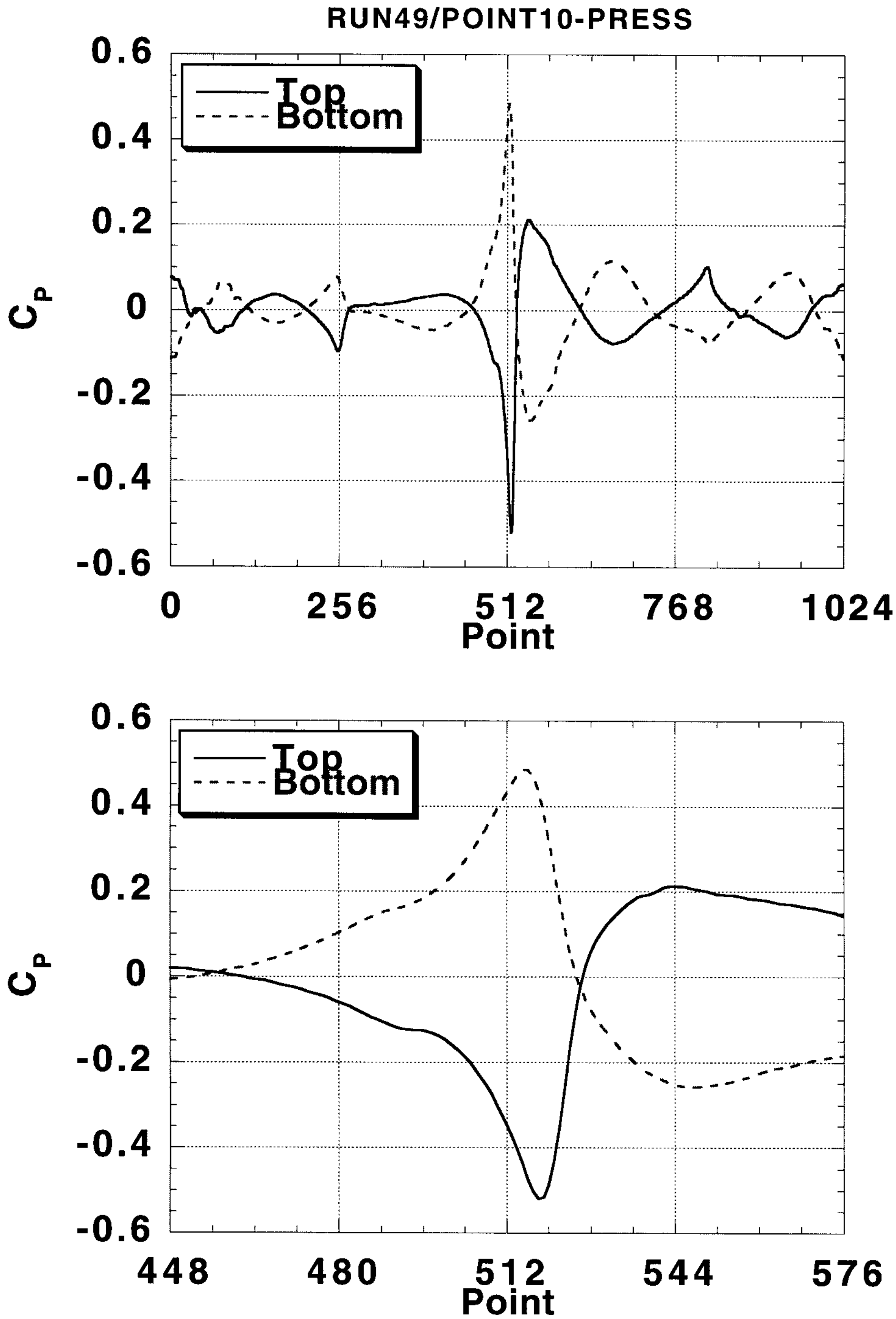
RUN49/POINT10-PRESS
Top
Bottom
0.6
0.4
0.2
0
-0.2
-0.4
-0.6
C_P
0
256
512
768
1024
Point
Top
Bottom
0.6
0.4
0.2
0
-0.2
-0.4
-0.6
C_P
448
480
512
544
576
Point

APPENDIX B-3

RUN 55 / POINT 6

α_V = +12°

z_V/c = 0

x_m = 0

RPM = 2114

M_{tip} = 0.714

θ_C = -0.11°

μ = 0.198

C_T/σ = -0.0034

T_T = 50.2 °F

a_0 = 1104.74 ft/sec

p_S = -0.327 psi

ρ = 0.002405 slug/ft^3

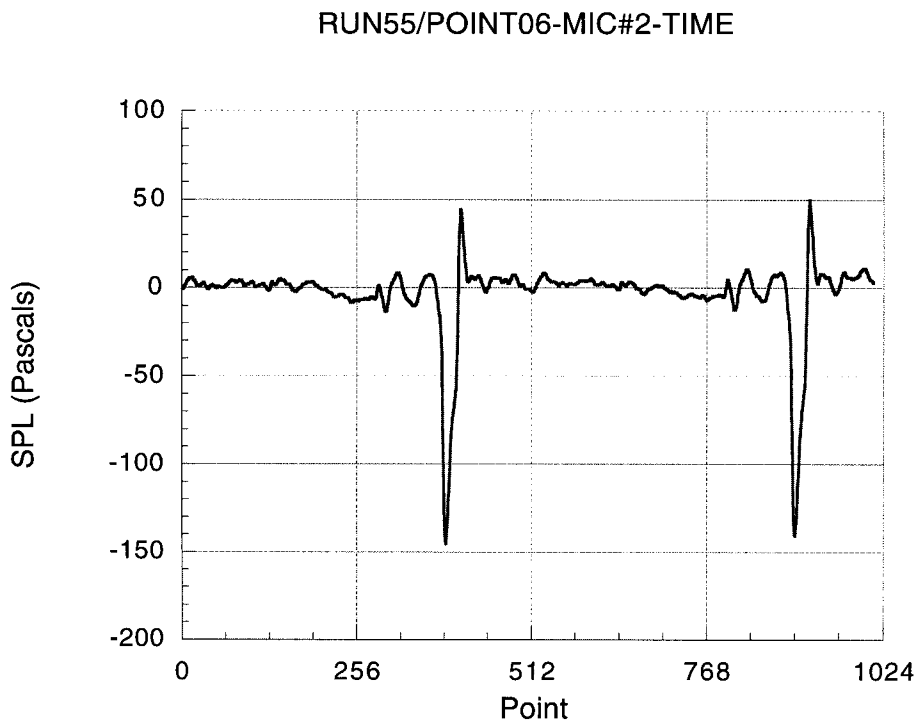
RUN55/POINT06-MIC#2-TIME
100
50
0
-50
-100
-150
-200
SPL (Pascals)
0
256
512
768
1024
Point

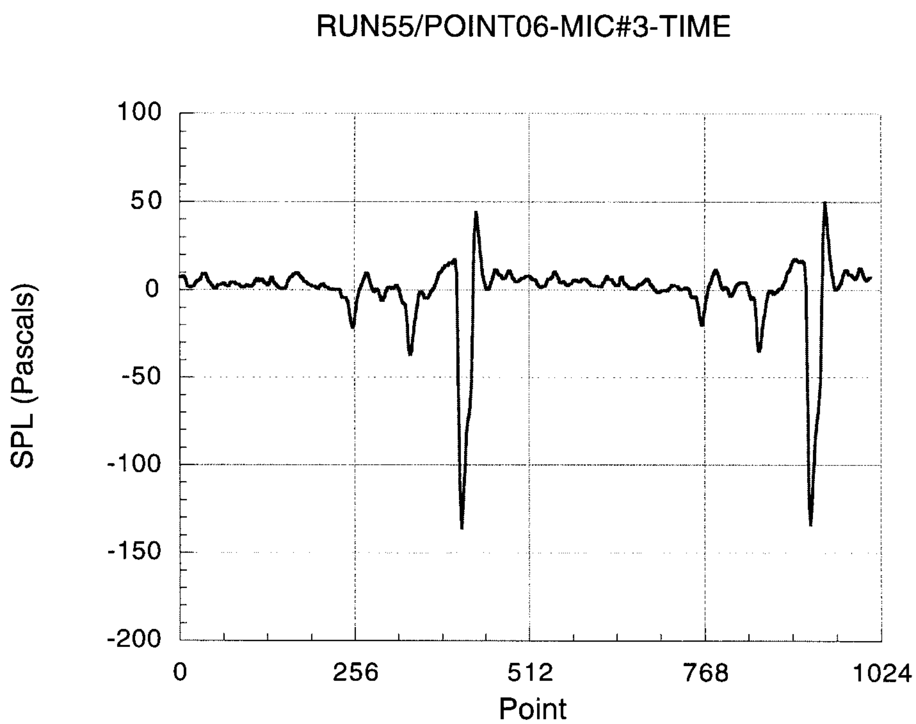
RUN55/POINT06-MIC#3-TIME
100
50
0
-50
-100
-150
-200
SPL (Pascals)
0
256
512
768
1024
Point

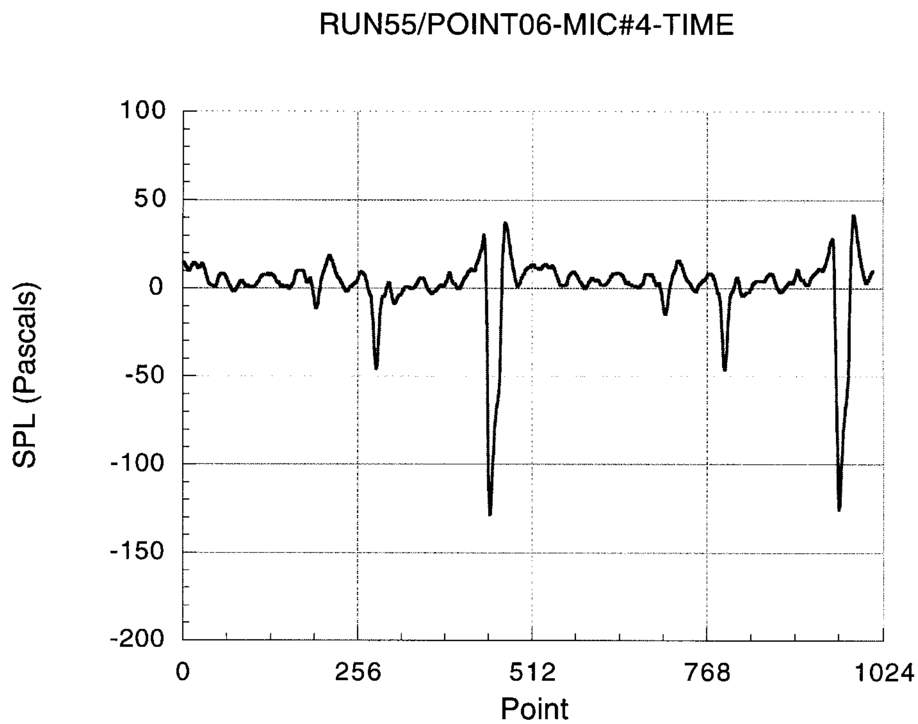
RUN55/POINT06-MIC#4-TIME
100
50
0
-50
-100
-150
-200
SPL (Pascals)
0
256
512
768
1024
Point

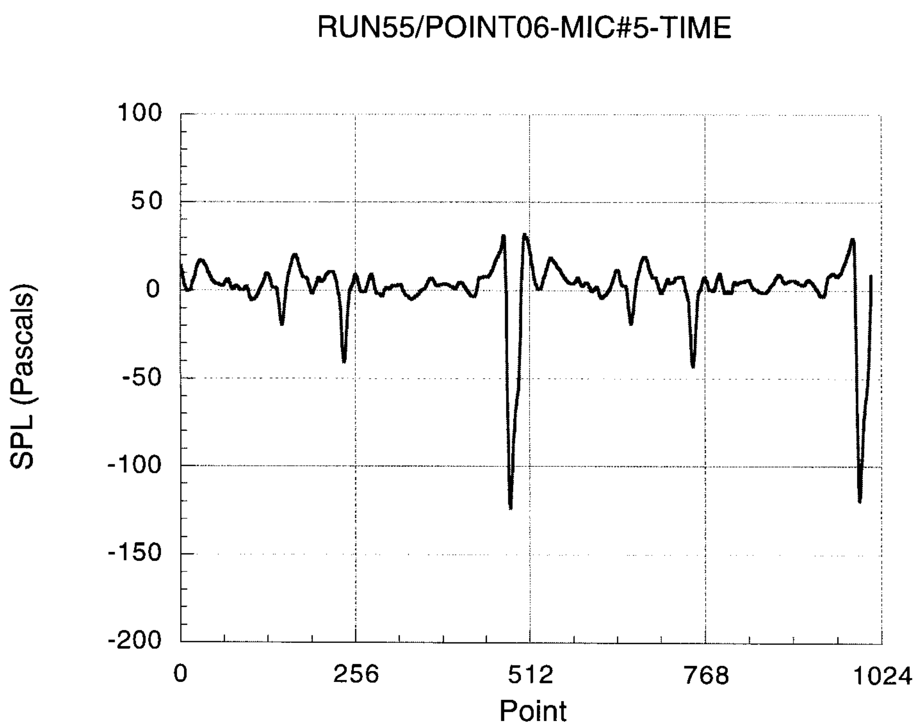
RUN55/POINT06-MIC#5-TIME
100
50
0
-50
-100
-150
-200
SPL (Pascals)
0
256
512
768
1024
Point

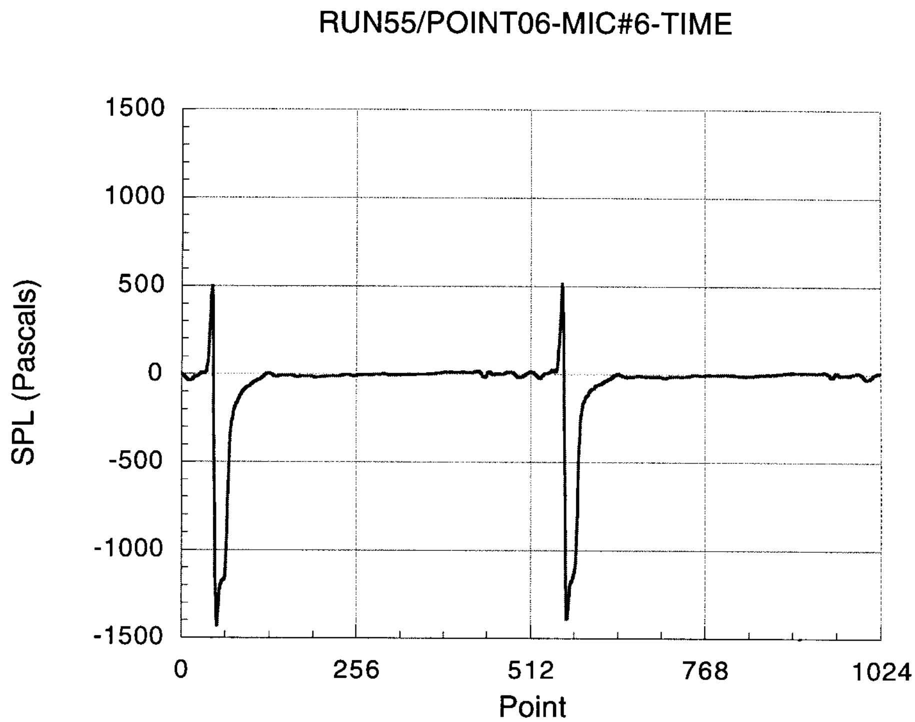
RUN55/POINT06-MIC#6-TIME
1500
1000
500
0
-500
-1000
-1500
SPL (Pascals)
0
256
512
768
1024
Point

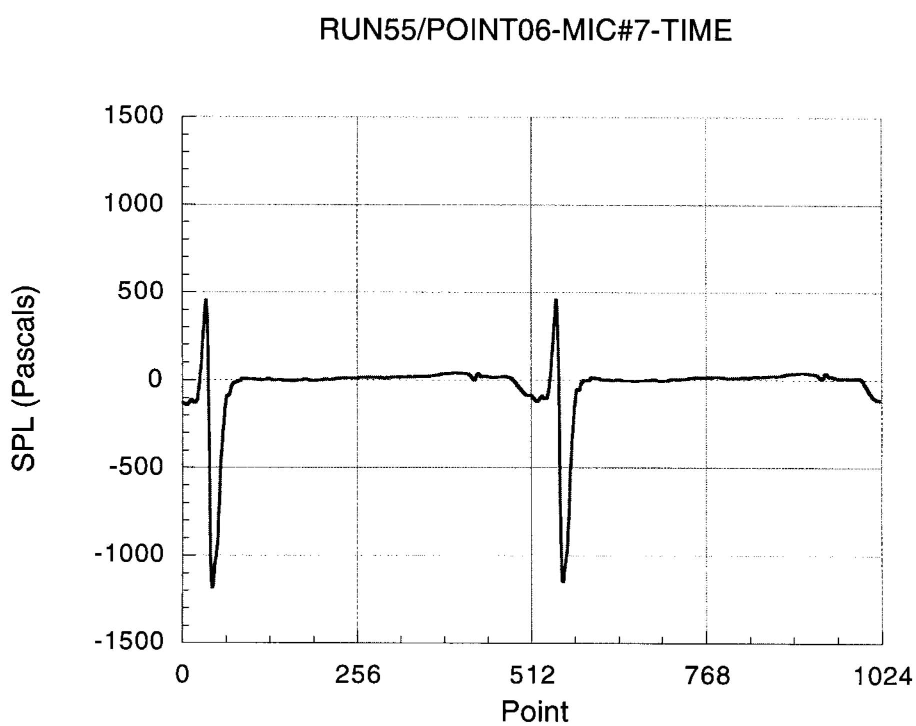
RUN55/POINT06-MIC#7-TIME
1500
1000
500
0
-500
-1000
-1500
SPL (Pascals)
0
256
512
768
1024
Point

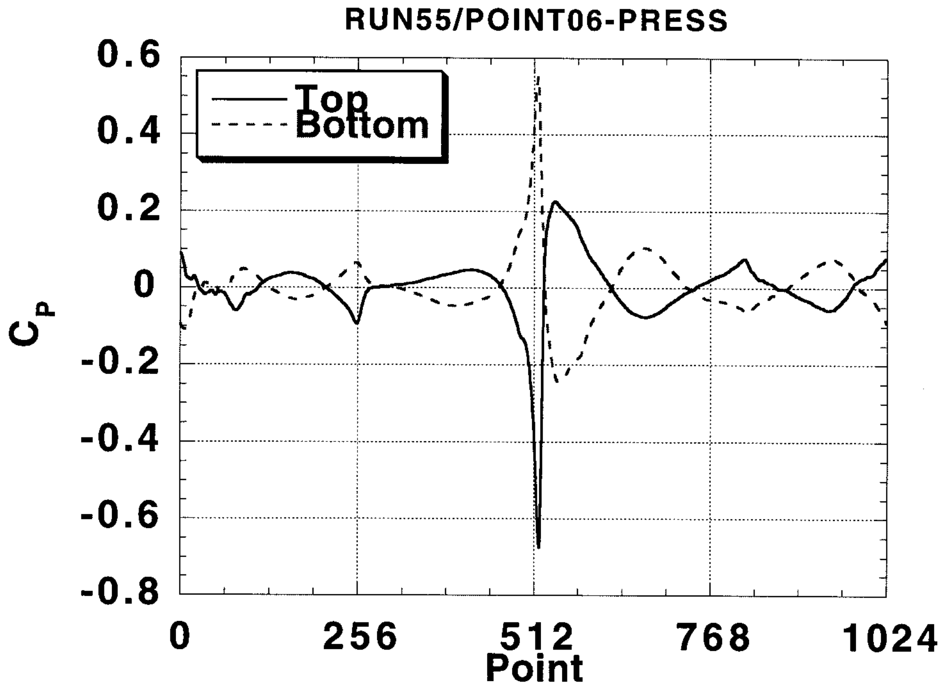
RUN55/POINT06-PRESS
Top
Bottom
C_P
Point
0.6
0.4
0.2
0
-0.2
-0.4
-0.6
-0.8
0
256
512
768
1024

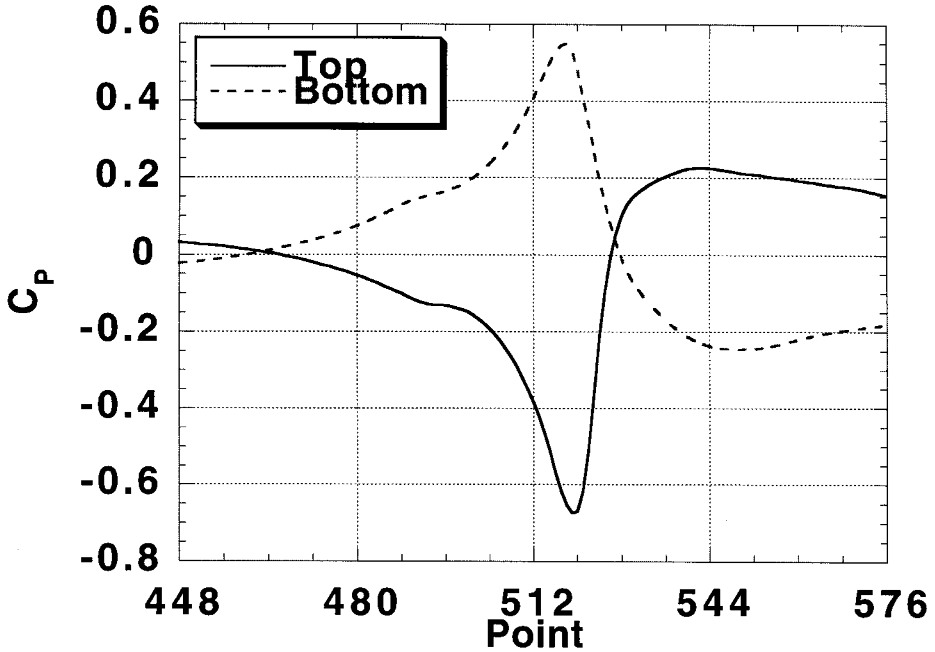
Top
Bottom
C_P
Point
0.6
0.4
0.2
0
-0.2
-0.4
-0.6
-0.8
448
480
512
544
576

APPENDIX B-4

RUN 55 / POINT 8

α_V = +12°	z_V/c = -0.125
x_m = 0	RPM = 2115
M_{tip} = 0.715	θ_C = -0.11°
μ = 0.198	C_T/σ = -0.0031
T_T = 49.6 °F	a_0 = 1104.09 ft/sec
p_S = -0.327 psi	ρ = 0.002407 slug/ft^3

RUN55/POINT08-MIC#2-TIME

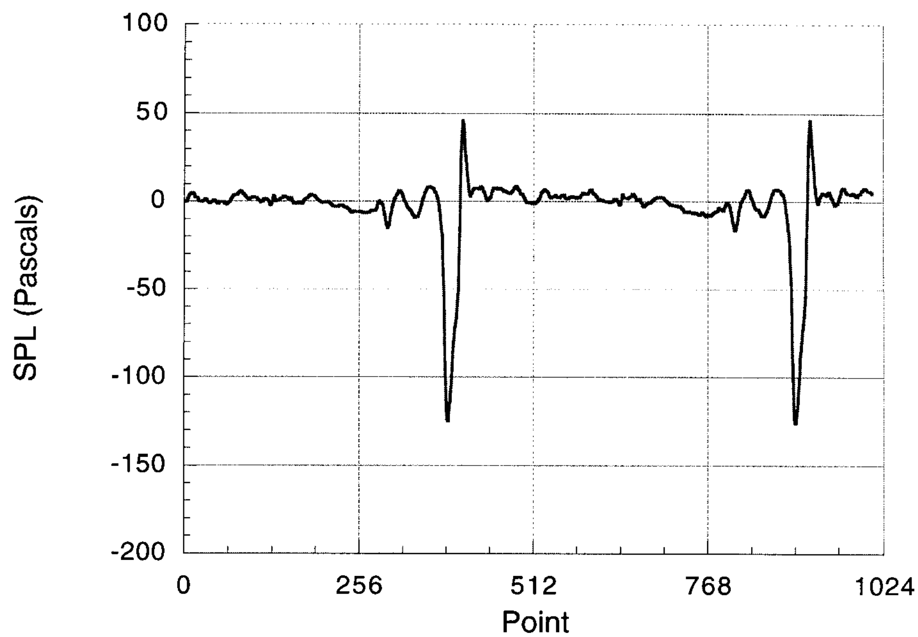

RUN55/POINT08-MIC#3-TIME

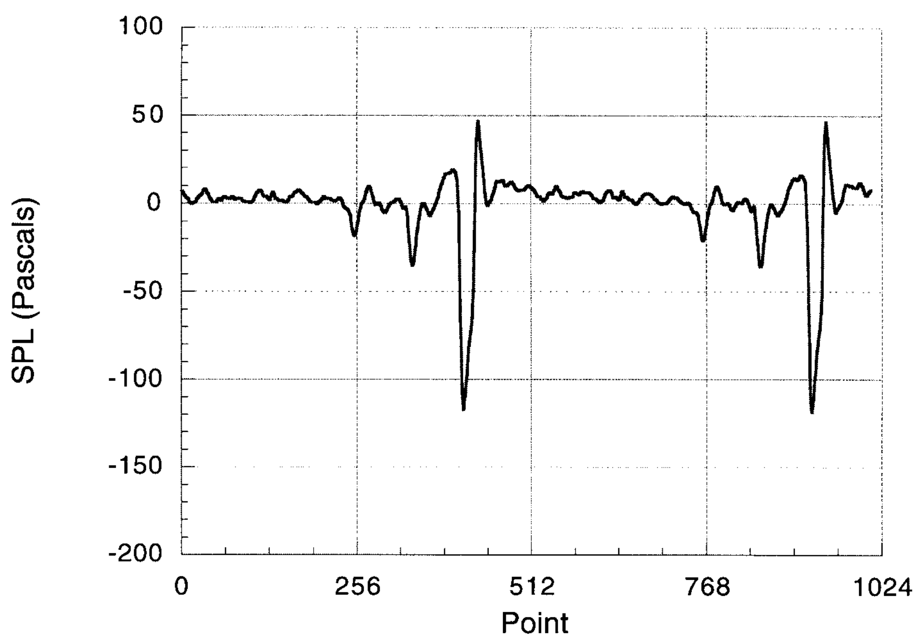

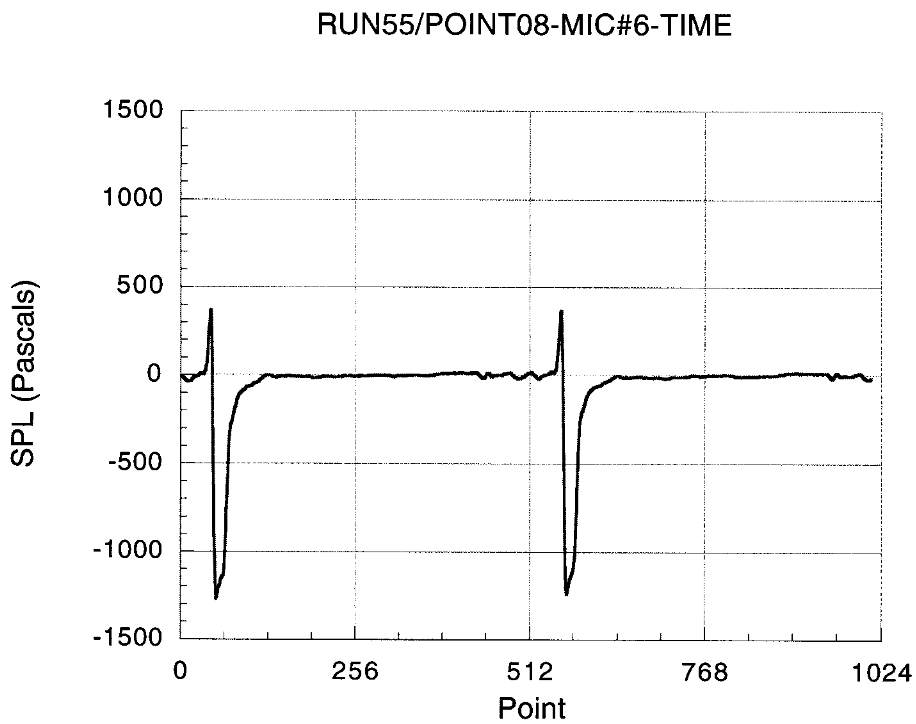
RUN55/POINT08-MIC#6-TIME
1500
1000
500
0
-500
-1000
-1500
SPL (Pascals)
0
256
512
768
1024
Point

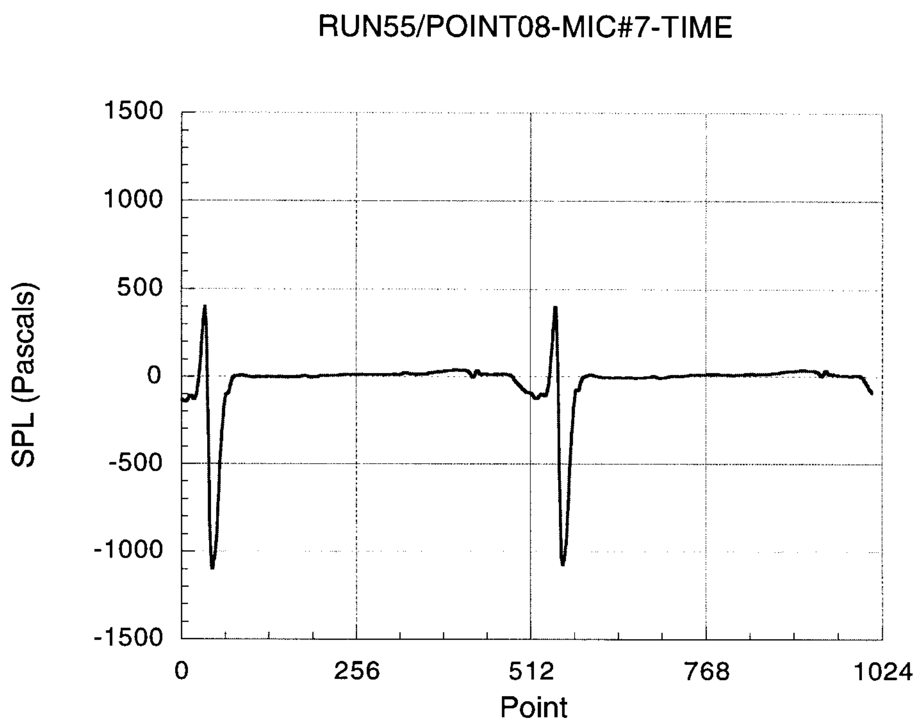
RUN55/POINT08-MIC#7-TIME
1500
1000
500
0
-500
-1000
-1500
SPL (Pascals)
0
256
512
768
1024
Point

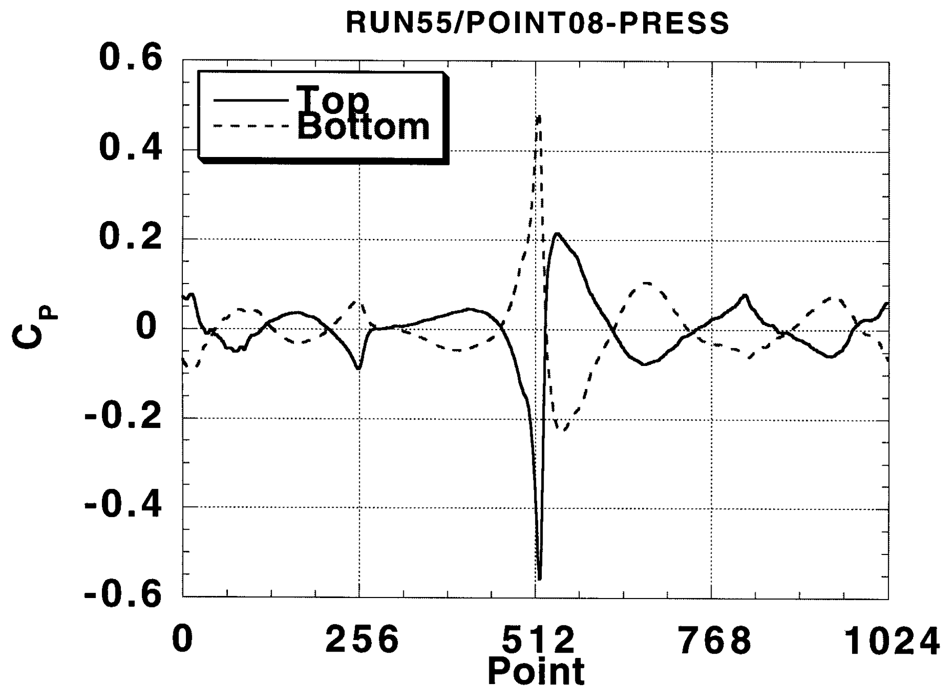

RUN55/POINT08-PRESS
Top
Bottom
0.6
0.4
0.2
0
-0.2
-0.4
-0.6
C_P
0
256
512
768
1024
Point

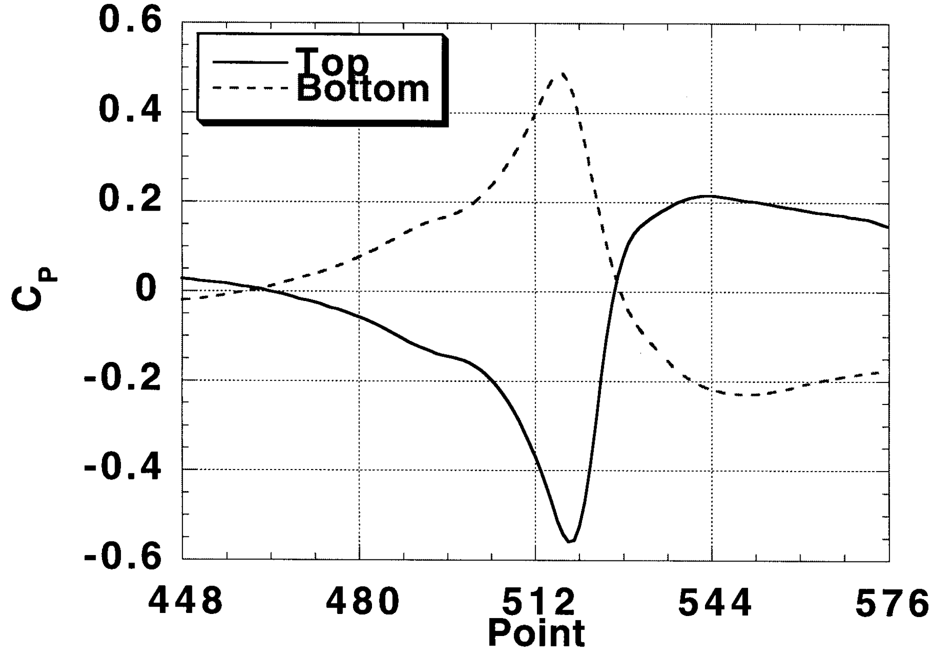

Top
Bottom
0.6
0.4
0.2
0
-0.2
-0.4
-0.6
C_P
448
480
512
544
576
Point

APPENDIX B-5

RUN 55 / POINT 7

α_V = +12°

x_m = 0

M_{tip} = 0.715

μ = 0.198

T_T = 49.8 °F

p_S = -0.327 psi

z_V/c = -0.25

RPM = 2116

θ_C = -0.11°

C_T/σ = -0.0033

a_0 = 1104.31 ft/sec

ρ = 0.002406 slug/ft^3

RUN55/POINT07-MIC#2-TIME

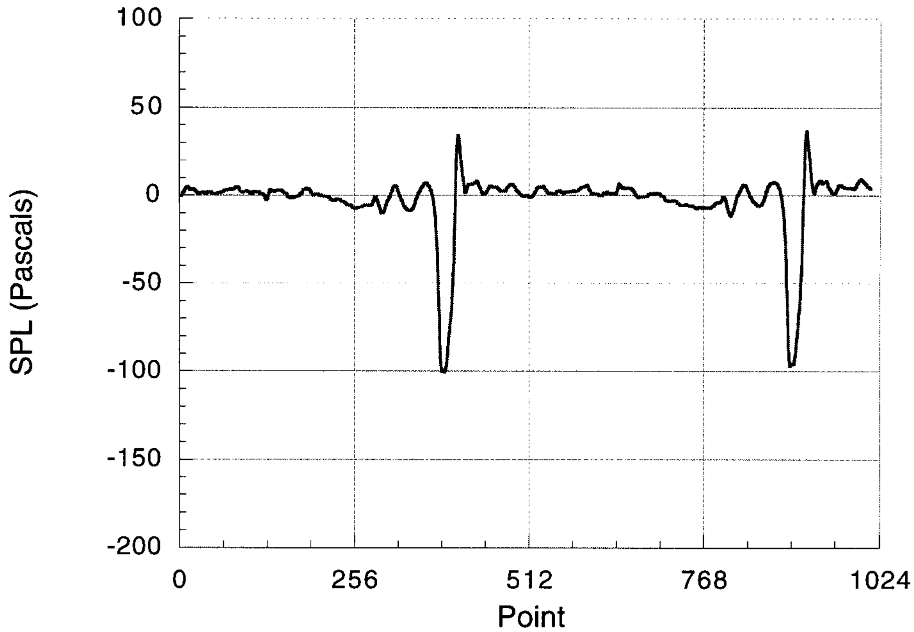

RUN55/POINT07-MIC#3-TIME

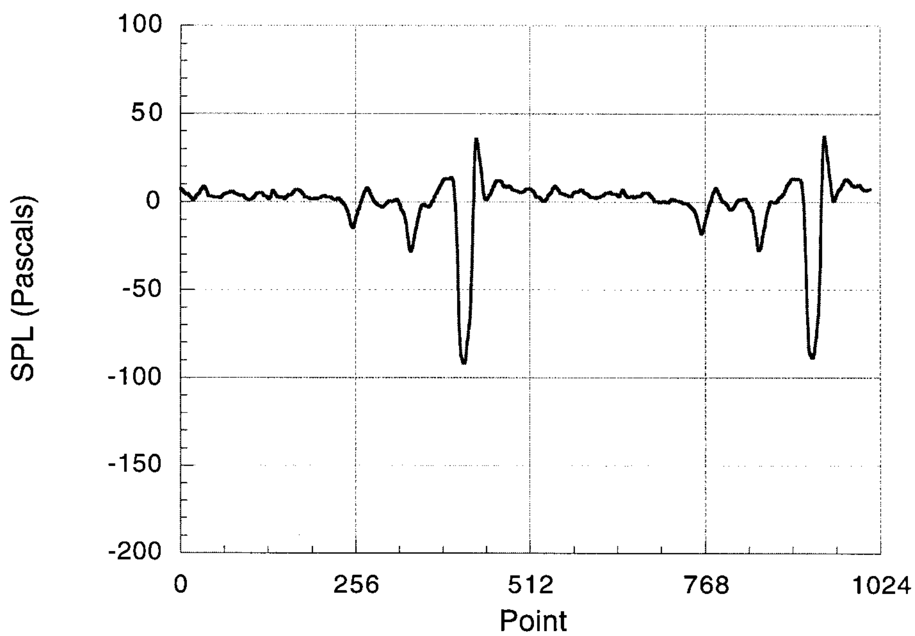

RUN55/POINT07-MIC#4-TIME

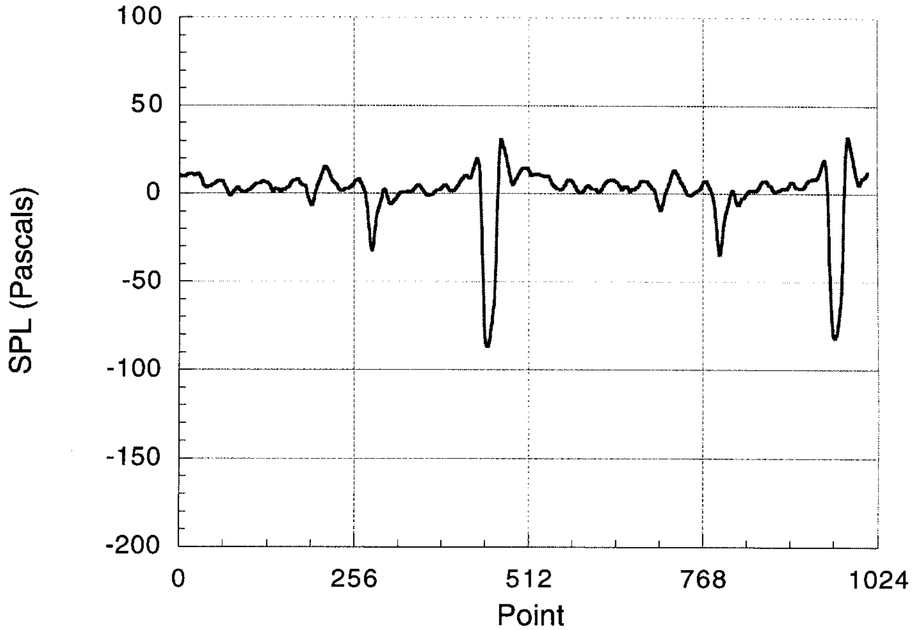

RUN55/POINT07-MIC#5-TIME

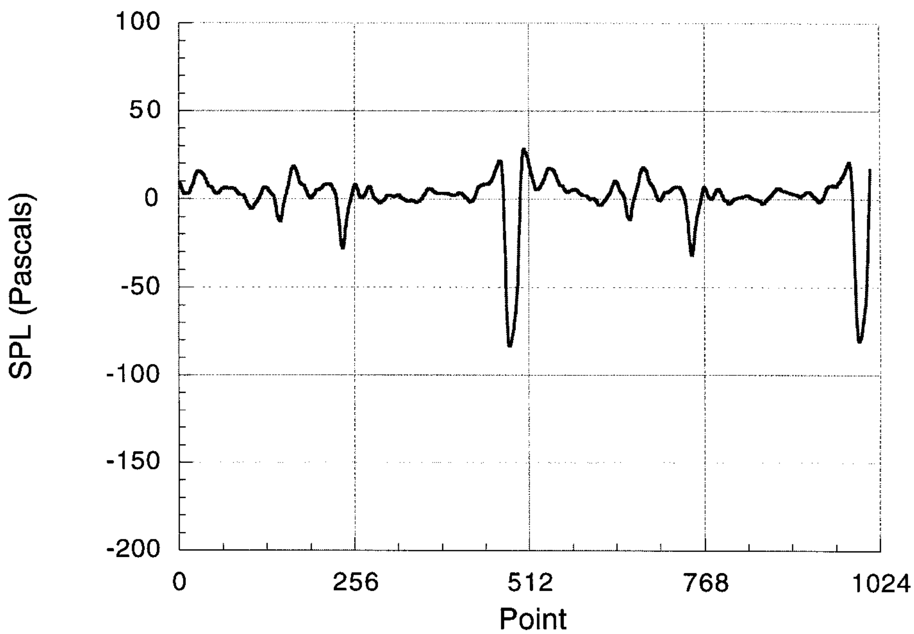

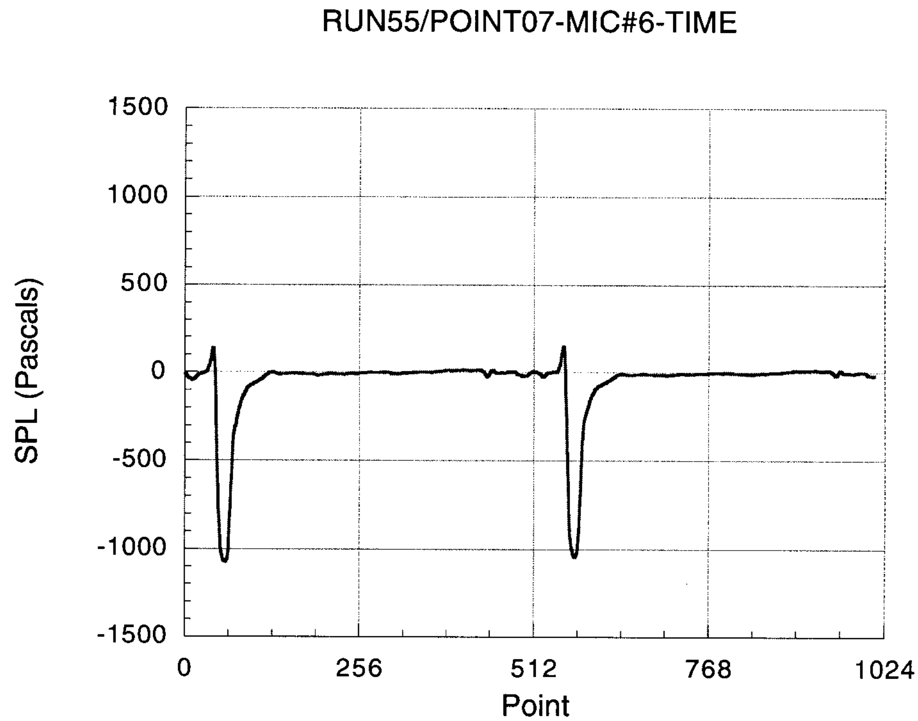

RUN55/POINT07-MIC#6-TIME
1500
1000
500
0
-500
-1000
-1500
SPL (Pascals)
0
256
512
768
1024
Point

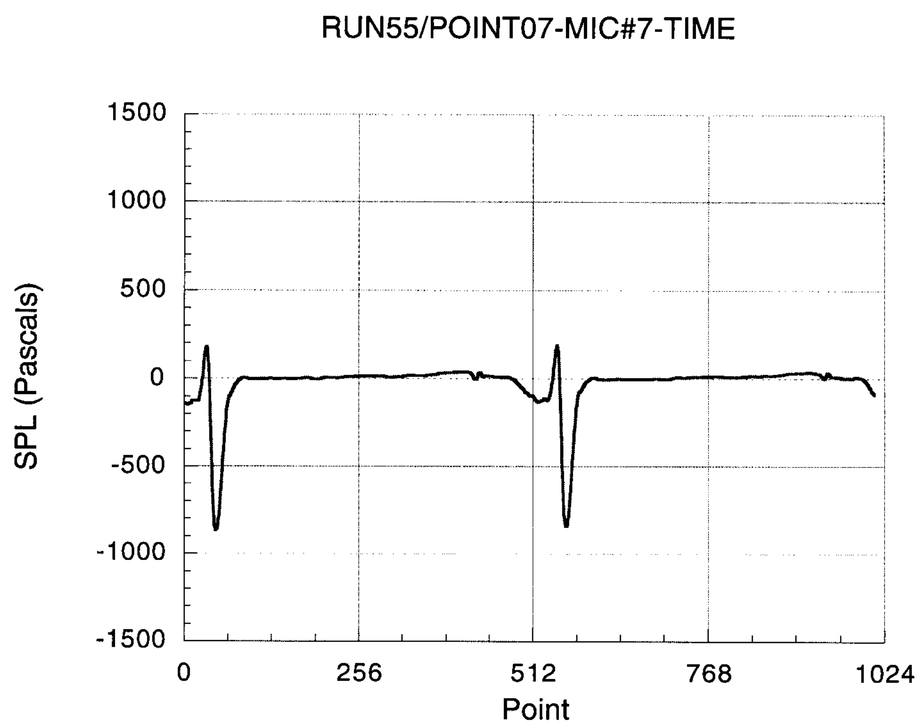

RUN55/POINT07-MIC#7-TIME
1500
1000
500
0
-500
-1000
-1500
SPL (Pascals)
0
256
512
768
1024
Point

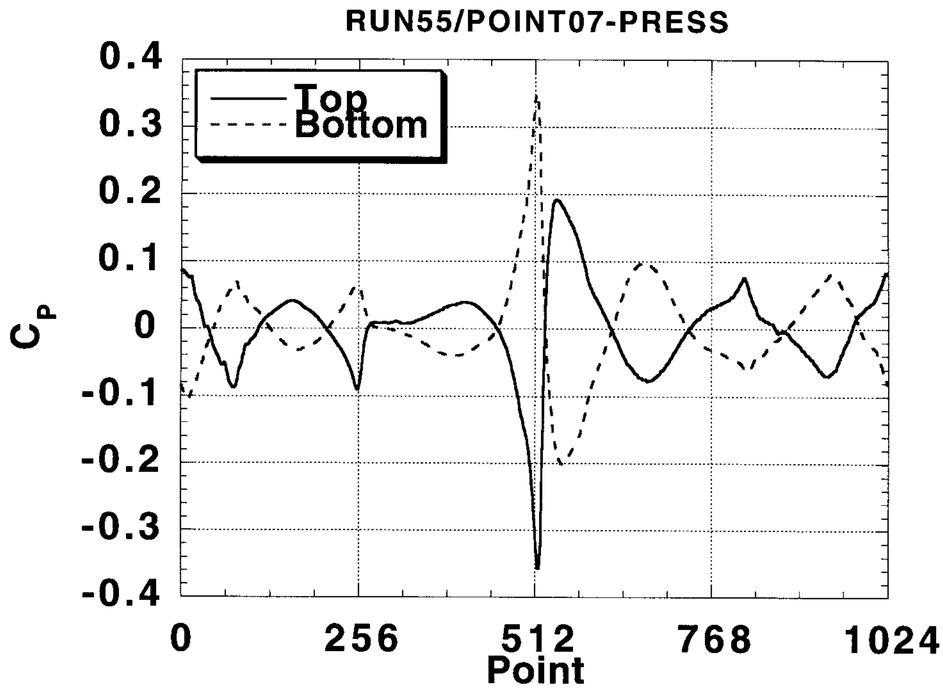

RUN55/POINT07-PRESS
Top
Bottom
0.4
0.3
0.2
0.1
0
-0.1
-0.2
-0.3
-0.4
C_P
0
256
512
768
1024
Point

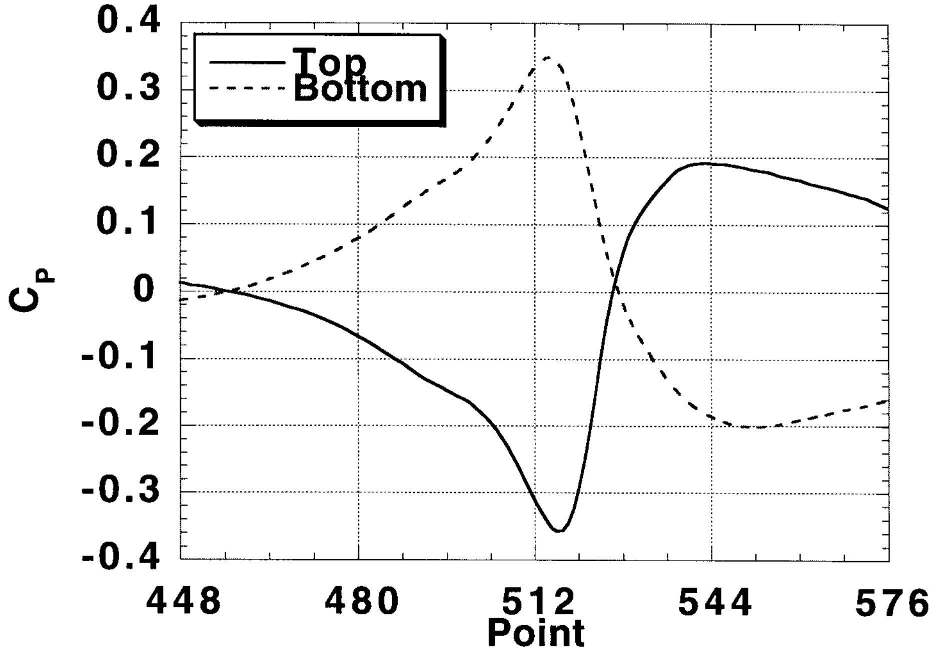

Top
Bottom
0.4
0.3
0.2
0.1
0
-0.1
-0.2
-0.3
-0.4
C_P
448
480
512
544
576
Point

APPENDIX B-6

<u>RUN 49 / POINT 13</u>

α_V = +12°

z_V/c = -0.375

x_m = 0

RPM = 2134

M_{tip} = 0.715

θ_C = -0.23°

μ = 0.198

C_T/σ = -0.0035

T_T = 58.8 °F

a_0 = 1114.01 ft/sec

p_S = -0.237 psi

ρ = 0.002359 slug/ft^3

NO ACOUSTIC DATA

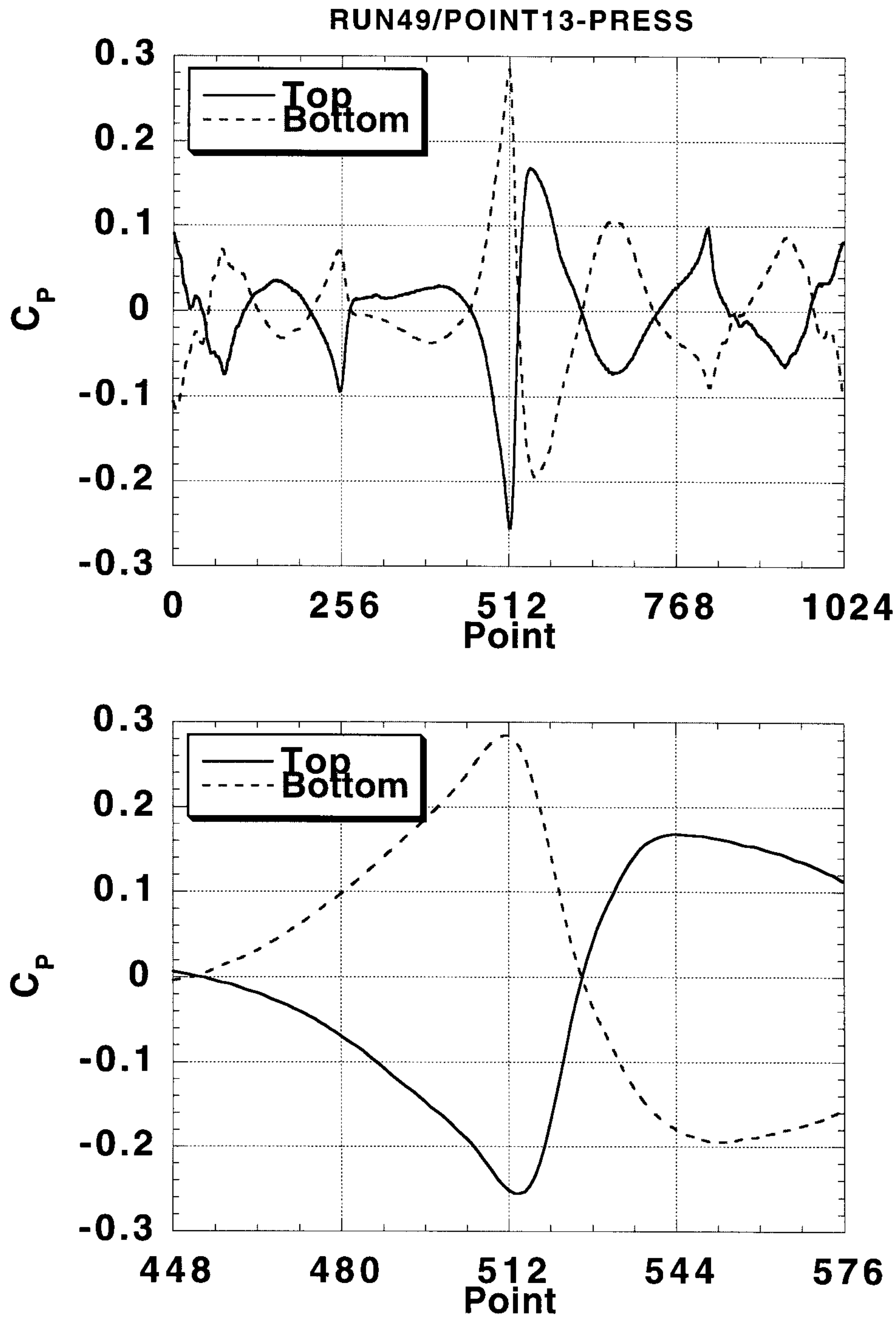
RUN49/POINT13-PRESS
Top
Bottom
C_P
0.3
0.2
0.1
0
-0.1
-0.2
-0.3
0
256
512
768
1024
Point
Top
Bottom
C_P
0.3
0.2
0.1
0
-0.1
-0.2
-0.3
448
480
512
544
576
Point

APPENDIX B-7

RUN 49 / POINT 14

α_V = +12°	z_V/c = -0.525
x_m = 0	RPM = 2133
M_{tip} = 0.714	θ_C = -0.25°
μ = 0.198	C_T/σ = -0.0034
T_T = 58.8 °F	a_0 = 1114.01 ft/sec
p_S = -0.237 psi	ρ = 0.002359 slug/ft^3

RUN49/POINT14-MIC#2-TIME

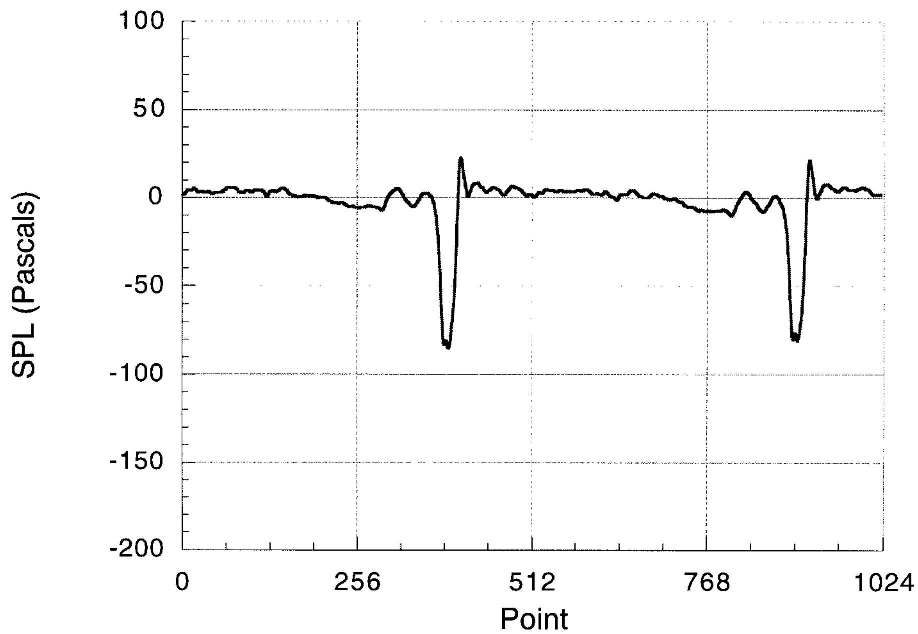

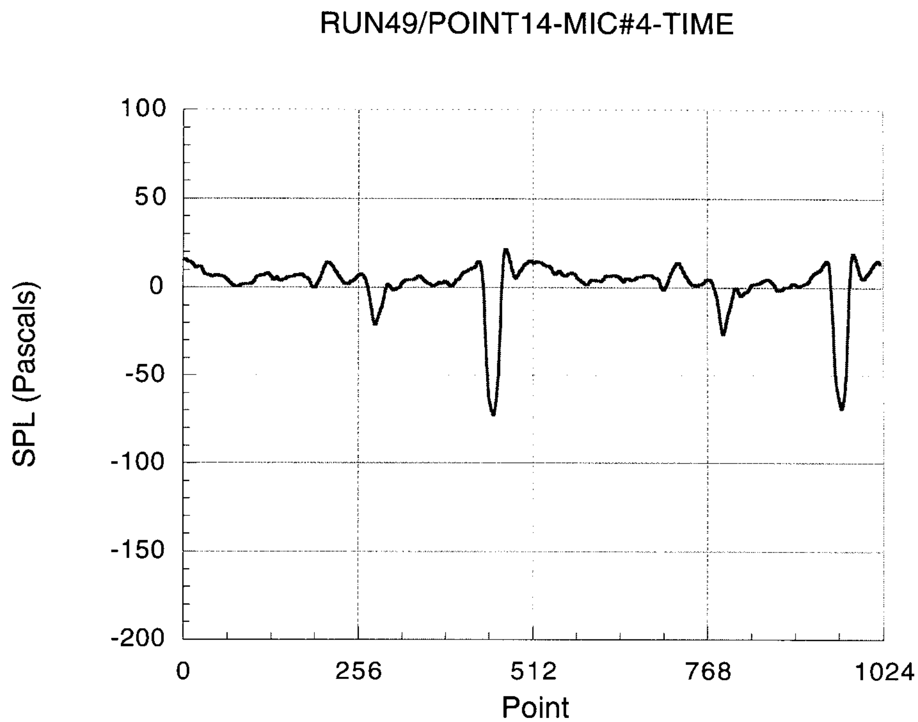
RUN49/POINT14-MIC#4-TIME
100
50
0
-50
-100
-150
-200
SPL (Pascals)
0
256
512
768
1024
Point

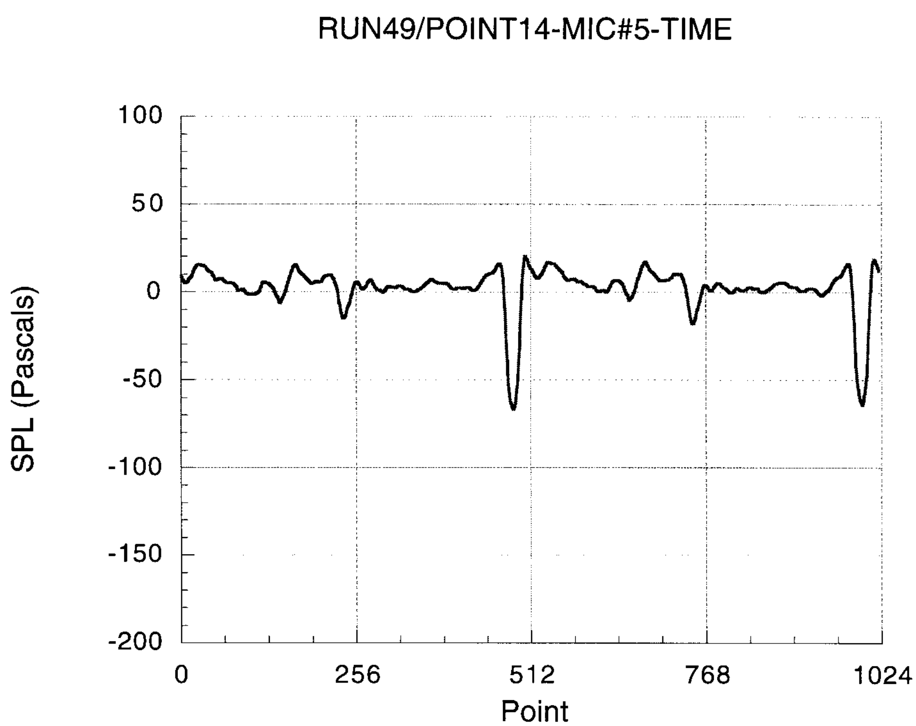
RUN49/POINT14-MIC#5-TIME
100
50
0
-50
-100
-150
-200
SPL (Pascals)
0
256
512
768
1024
Point

RUN49/POINT14-MIC#6-TIME

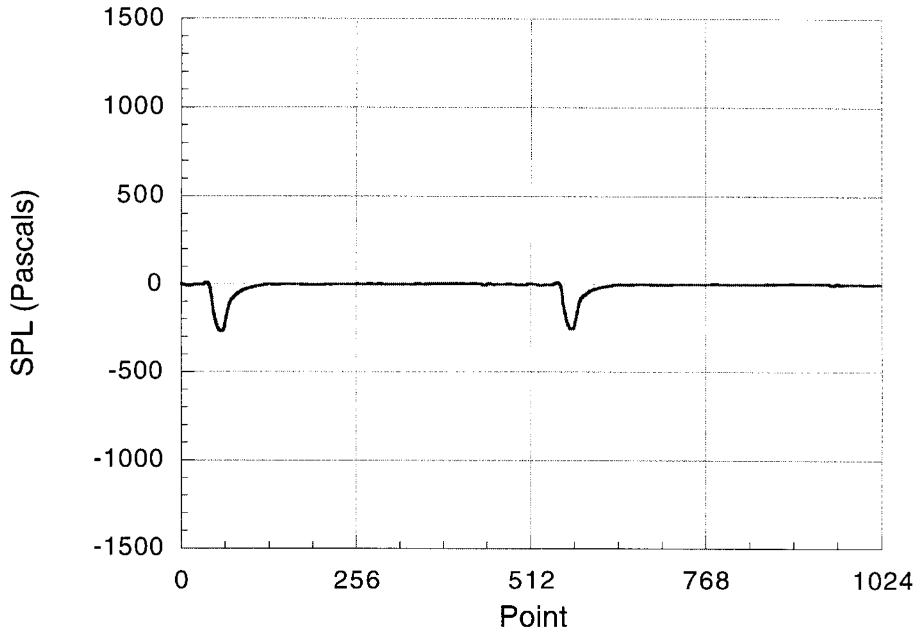

RUN49/POINT14-MIC#7-TIME

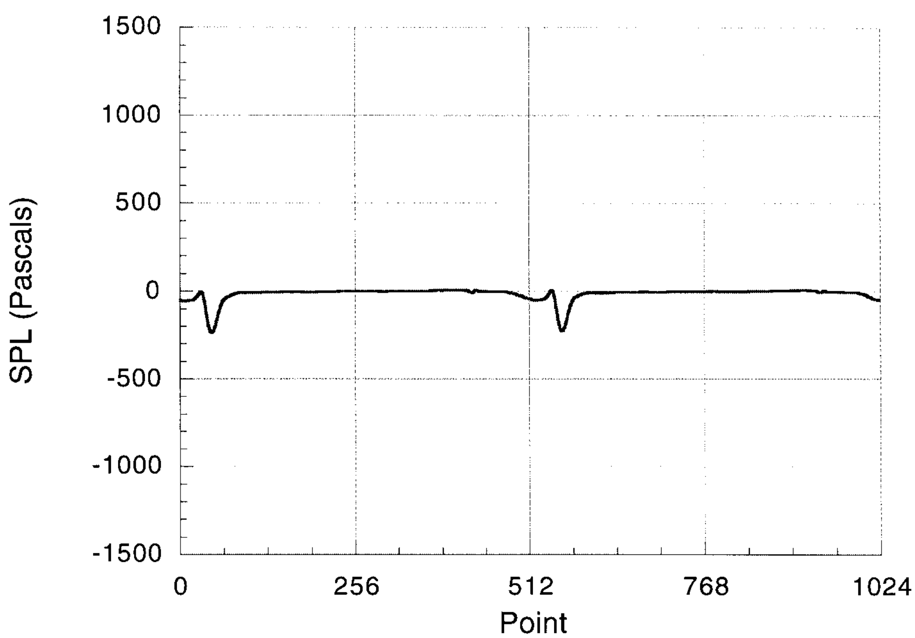

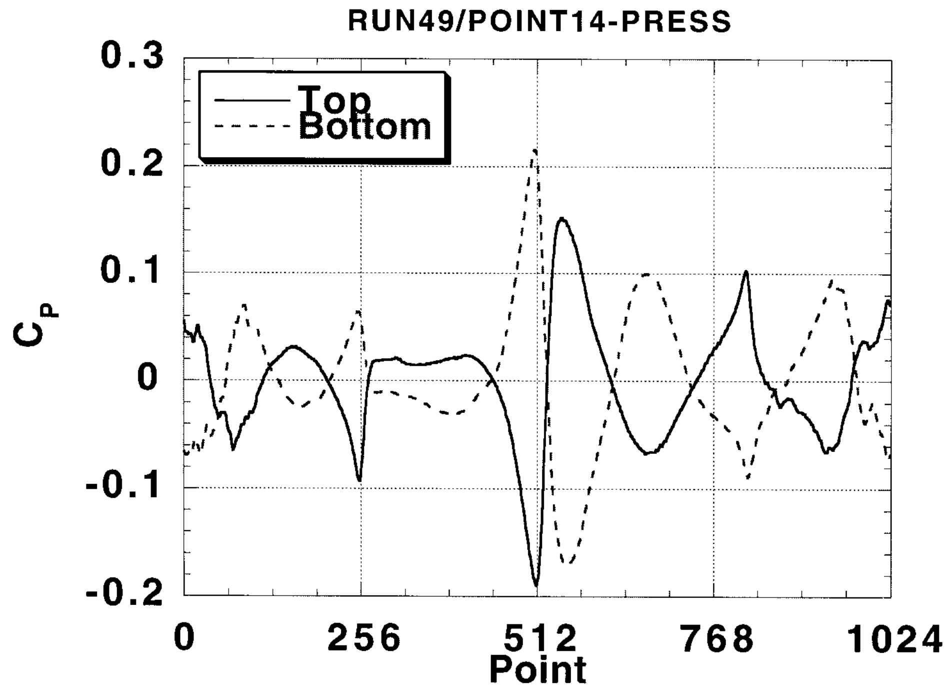
RUN49/POINT14-PRESS
Top
Bottom
0.3
0.2
0.1
0
-0.1
-0.2
C_P
0
256
512
768
1024
Point

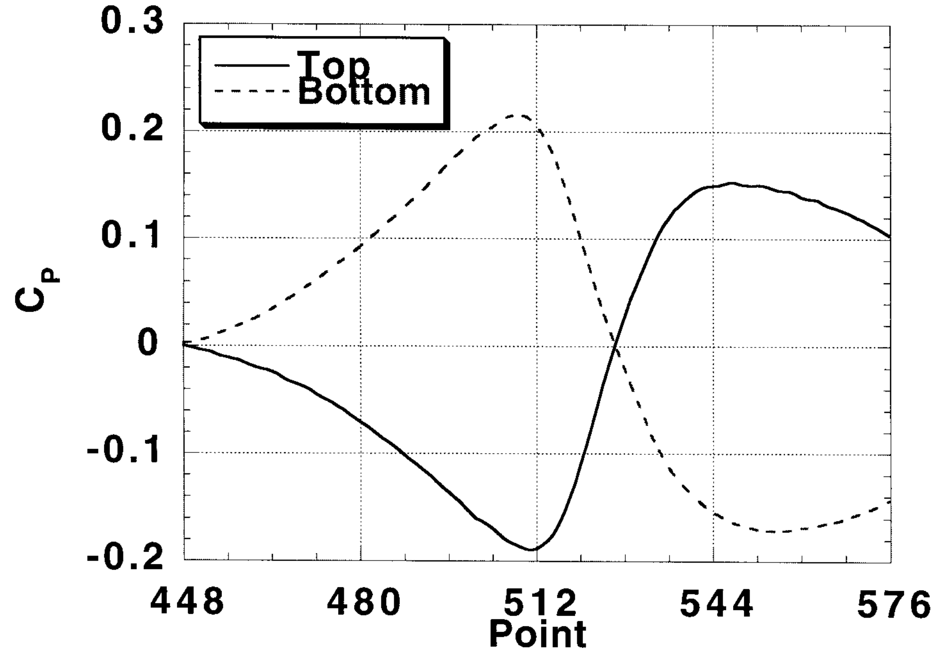
Top
Bottom
0.3
0.2
0.1
0
-0.1
-0.2
C_P
448
480
512
544
576
Point

APPENDIX C

The enclosed computer CD-ROM contains the data files of Appendices A and B in text format. The CD-ROM is in ISO 9660 format and should be readable by the majority of computers.

For the acoustic data there is a separate file for each Run/Point and Microphone as indicated by the file names. These files are in two columns separated by a tab character, each line being terminated by a carriage return. The first column is the data point (nominally 1024 points per revolution; see discussion in the "Data Processing" section). The second column is the Sound Pressure in Pascals. An example printout is included.

For the blade pressure data, there is a separate file for each Run/Point, indicated by the file names. The files are in tab delimited columns. Each file has 60 columns, one for each pressure transducer, and 1024 rows, one for each azimuth point. The columns of the pressure transducer data are ordered as follows:

1 - 10	r/R = 0.946, top
11 - 20	bottom
21 - 30	r/R = 0.876, top
31 - 40	bottom
41 - 50	r/R = 0.772, top
51 - 60	bottom

The pressure data are in units of nondimensional C_P. An example printout is included. (Note that in this example printout, the data appear in six columns to accommodate page width limitations. In this printed format, each group of 60 numbers (in 6 columns by 10 rows) represents one azimuth point, and will appear on a single row in the file.)

Example printout of acoustic data file

1.000000	-0.003857
2.000000	0.819274
3.000000	1.779594
4.000000	2.328348
5.000000	2.739914
6.000000	3.288668
7.000000	3.700234
8.000000	4.386177
9.000000	4.934931
10.000000	5.346496
11.000000	5.758062
12.000000	6.444005
13.000000	7.541513
14.000000	7.953079
15.000000	8.090267

•
•
•

1007.000000	3.563045
1008.000000	3.014291
1009.000000	2.465537
1010.000000	2.191159
1011.000000	1.779594
1012.000000	1.505217
1013.000000	1.368028
1014.000000	1.230840
1015.000000	0.956463
1016.000000	0.682085
1017.000000	-0.003857
1018.000000	-0.552612
1019.000000	-1.101366

Example printout of blade pressure data file

-0.1052	0.0182	0.0015	0.0118	0.0014
0.0015	0.0001	0.0025	0.0010	0.0025
-0.0068	-0.0099	-0.0185	-0.0021	-0.0015
-0.0024	-0.0011	-0.0010	-0.0010	-0.0453
0.0472	0.0348	0.0179	0.0079	0.0030
0.0050	0.0029	0.0004	-0.0013	-0.0038
-0.0395	-0.0224	-0.0049	-0.0136	-0.0116
-0.0051	-0.0031	-0.0003	0.0078	0.0070
0.0828	-0.0150	0.0274	0.0121	0.0107
0.0071	0.0116	0.0066	0.0055	0.0031
-0.0926	-0.0595	-11.5343	-0.0267	-0.0193
-0.0140	-0.0086	-0.0060	-0.0021	-0.0029
-0.1021	0.0168	0.0012	0.0125	0.0011
0.0018	-0.0015	0.0010	0.0004	0.0015
-0.0044	-0.0058	-0.0168	-0.0012	-0.0013
-0.0019	-0.0007	-0.0007	0.0000	-0.0432
0.0399	0.0306	0.0143	0.0087	0.0020
0.0034	0.0013	0.0002	-0.0016	-0.0037
-0.0362	-0.0198	-0.0048	-0.0121	-0.0102
-0.0052	-0.0026	0.0006	0.0081	0.0071
0.0789	0.0216	0.0282	0.0128	0.0094
0.0063	0.0101	0.0055	0.0043	0.0024
-0.0937	-0.0571	-11.3408	-0.0250	-0.0180
-0.0127	-0.0085	-0.0047	-0.0010	-0.0014
.				
.				
.				
-0.3486	0.0113	-0.0026	0.0056	-0.0023
0.0028	0.0002	0.0003	-0.0003	0.0001
-0.0124	-0.0181	-0.0223	-0.0043	-0.0027
-0.0031	-0.0015	-0.0017	-0.0007	-0.1511
0.0474	0.0305	0.0137	0.0077	0.0023
0.0015	0.0001	0.0004	0.0000	-0.0018
-0.0456	-0.0285	-0.0122	-0.0155	-0.0131
-0.0060	-0.0044	-0.0012	0.0089	0.0080
0.0910	-0.0434	0.0277	0.0145	0.0094
0.0118	0.0126	0.0078	0.0061	0.0039
-0.0982	-0.0631	-20.4493	-0.0291	-0.0213
-0.0162	-0.0134	-0.0077	-0.0061	-0.0052
-0.3377	0.0098	-0.0020	0.0059	-0.0013
0.0007	0.0004	-0.0006	-0.0018	0.0018
-0.0094	-0.0144	-0.0207	-0.0035	-0.0020
-0.0028	-0.0015	-0.0016	-0.0014	-0.1488
0.0418	0.0262	0.0125	0.0064	0.0029
-0.0008	-0.0005	-0.0002	-0.0013	-0.0024
-0.0424	-0.0259	-0.0120	-0.0147	-0.0131
-0.0056	-0.0041	-0.0006	0.0084	0.0046
0.0887	-0.0943	0.0285	0.0142	0.0091
0.0105	0.0102	0.0067	0.0049	0.0042
-0.0940	-0.0621	-20.2389	-0.0274	-0.0212
-0.0156	-0.0120	-0.0072	-0.0049	-0.0044

REPORT DOCUMENTATION PAGE

Form Approved
OMB No. 0704-0188

1. AGENCY USE ONLY ***(Leave blank)***

2. REPORT DATE
July 1999

3. REPORT TYPE AND DATES COVERED
Technical Memorandum

4. TITLE AND SUBTITLE
An Experimental Study of Parallel Blade-Vortex Interaction Aerodynamics and Acoustics Utilizing an Independently Generated Vortex

5. FUNDING NUMBERS
581-10-12

6. AUTHOR(S)
C. Kitaplioglu, F. X. Caradonna, and M. McCluer

7. PERFORMING ORGANIZATION NAME(S) AND ADDRESS(ES)
Ames Research Center
Moffett Field, CA 94035-1000

8. PERFORMING ORGANIZATION REPORT NUMBER
A-99V0031

9. SPONSORING/MONITORING AGENCY NAME(S) AND ADDRESS(ES)
National Aeronautics and Space Administration
Washington, DC 20546-0001

10. SPONSORING/MONITORING AGENCY REPORT NUMBER
NASA/TM–1999-208790

11. SUPPLEMENTARY NOTES
Point of Contact: C. Kitaplioglu, Ames Research Center, MS T12B, Moffett Field, CA 94035-1000
(650) 604-6679

12a. DISTRIBUTION/AVAILABILITY STATEMENT
Unclassified — Unlimited
Subject Category 05 Distribution: Standard
Availability: NASA CASI (301) 621-0390

12b. DISTRIBUTION CODE

13. ABSTRACT ***(Maximum 200 words)***

This report presents results from an experimental study of rotor blade-vortex interaction (BVI) aerodynamics and acoustics. The experiment utilized an externally generated vortex interacting with a two-bladed rotor operating at zero thrust to minimize the influence of the rotor's own wake. The rotor blades were instrumented with a total of 60 absolute pressure transducers at three spanwise and ten chordwise stations on both the upper and lower surfaces. Acoustic data were obtained with fixed near-field microphones as well as a movable array of far-field microphones. The test was carried out in the acoustically treated test section of the NASA Ames 80- by 120-Foot Wind Tunnel. Several parameters that influence BVI, such as vortex-rotor separation distance, vortex strength, and vortex sense (swirl direction), as well as rotor tip Mach number and advance ratio, were varied. Simultaneous measurements were obtained of blade surface pressure distributions, near-field acoustics, and far-field acoustics during the vortex-blade encounters. A representative subset of the data is included in the Appendices. The entire reduced data set is included on the enclosed CD-ROM.

14. SUBJECT TERMS
Rotorcraft, Acoustics, Blade-vortex interaction

15. NUMBER OF PAGES
81

16. PRICE CODE
A05

17. SECURITY CLASSIFICATION OF REPORT	18. SECURITY CLASSIFICATION OF THIS PAGE	19. SECURITY CLASSIFICATION OF ABSTRACT	20. LIMITATION OF ABSTRACT
Unclassified	Unclassified		